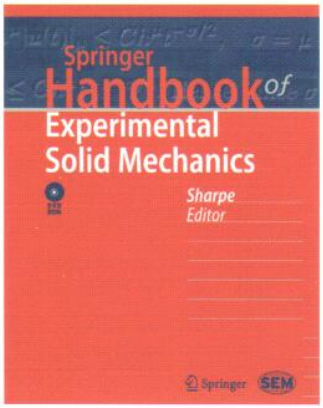

SPRINGER REFERENCE

Published in collaboration with the Society for Experimental Mechanics

SEM

Springer Handbook of Experimental Solid Mechanics

Editor: **William N. Sharpe, Jr.**, Johns Hopkins University

As a reference book, the Springer Handbook provides a comprehensive exposition of the techniques and tools of experimental mechanics. An informative introduction to each topic is provided, which advises the reader on suitable techniques for practical applications.

New exciting topics include biological materials, MEMS and NEMS, nanoindentation, digital photomechanics, photoacoustic characterization, and atomic force microscopy in experimental solid mechanics.

Written by international experts from top academic institutions as well as industry from across the globe, the **Springer Handbook of Experimental Solid Mechanics** features an extensive compilation of useful and up-to-date references. A detailed index and fully searchable DVD are included, complete with supplementary media.

Key Topics

- MEMS and NEMS
- Nanoindentation
- Geometric Moiré
- Photoacoustic Characterization of Materials
- Polymers and Viscoelasticity
- Hybrid Methods
- Electronic Packaging
- Thermoelastic Stress Analysis
- High Strain Rate and Impact Testing
- Speckle Methods
- X-ray Stress Analysis

Sample pages available at springer.com/engineering

Print
DVD 2008. Approx. 1400 p.
800 illus. in color.
With DVD-ROM with full contents
Hardcover
978-0-387-26883-5
► **$199.00**

eReference
978-0-387-30877-7
► **$199.00**

Print + eReference
978-0-387-34362-4
► **$249.00**

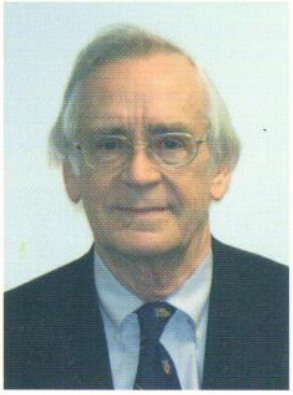

About the Editor

William N. Sharpe, Jr. holds the Alonzo G. Decker Chair in Mechanical Engineering at the Johns Hopkins University where he served as department chairman for 11-1/2 years. His early research focused on laser-based strain measurement over very short gage lengths to study plasticity and fracture behavior. The past fifteen years have been devoted to development and use of experimental methods to measure the mechanical properties of materials used in microelectromechanical systems. He is a Fellow and Past President of the Society for Experimental Mechanics from which he received the Murray Medal. The American Society of Mechanical Engineers awarded him the Nadai Award as well as Fellow grade. He has received an Alexander von Humboldt Award along with the Roe Award from the American Society of Engineering Education.

Table of Contents

35. Structural Testing Applications

Ashok Kumar Ghosh

This chapter addresses various aspects of testing of a structural system. The importance of the *management approach* to planning and performing structural tests (ST) is emphasized. When resources are limited, this approach becomes critical to the successful implementation of a testing program. The chapter starts with illustrations of some of the past structures that were built using concepts developed through testing. Most often, these structures were built even before the principles of engineering mechanics were understood. At present, due to the unprecedented expansion of computing power, numerical and experimental techniques are interchangeably used in simulating complex natural phenomena. Despite encouraging results from simulation and predictive modeling, structural testing is still a very valuable tool in the industrial development of product and process, and its success depends on judicious choice of testing method, instrumentation, data acquisition, and allocation of resources. A generic description of the current test equipment and types of measurements is included in this chapter. After careful selection, three case studies are included. The complexity involved with the modeling of structural steel retrieved from the collapse site of the World Trade Center (WTC) under high-rate and high-temperature conditions is highlighted in the first case study. The second case study highlights the importance of the planning phase in providing the basis for manageable and high-quality testing of concrete highway bridges. The final case study details the development of a lightweight automobile airbag from inception through innovation. This case study also illustrates the close ties between structural testing and numerical simulation. The chapter closes with examples of a few future structural systems, highlighting the complexity involved in their testing.

A structure is an engineered system that must fulfill multiple requirements. Testing of a structural system has a definite role to play in the overall process of development, be it in the context of developing new products or assessing existing products. The design-by-testing methodology (Fig. 35.1) seems to work well in this development process.

Testing expands the knowledge base regarding different parameters that influence the design and development. As one learns more about a particular process, one tends to cut efforts on physical testing to reduce time and cost, resulting in greater emphasis on predictive modeling. Three primary reasons attribute to such a shift in emphasis.

First, the unprecedented expansion of computing power in the last decade has enabled us to develop high-performance scientific computing hardware. Between the 1990s and the present, this computing speed has improved 20 times from 2 tera-operations per second (OPS) to 40 tera OPS. All these computational capabilities are ideal for supporting highly complex and interdisciplinary application-oriented developments.

Second, with these improved supercomputing capabilities, it is often possible to model a complex physical phenomenon. For most of the conventional problems, there is extraordinary agreement between the simulation and the real situation, thus making the requirement for experiments less important. The initiative *Engineering Sciences for Modeling and Simulations-Based Life-Cycle Engineering* is a collaborative research program by the National Science Foundation (NSF) and the Sandia National Laboratories (SNL) that focuses on advancing the fundamental knowledge needed to support advanced computer simulations. SNL is moving towards engineering processes in which decisions are based heavily on computational simulations, thus capitalizing on the available high-performance computing platforms. In the future, dominant use of analysis will be a part of the design process.

Third, engineering design and development through experimentation will be used as a fact-finding tool that allows one to understand the circumstances surrounding a given problem and the main variables controlling it. Characteristically, complex systems are nonlinear, coupled, and exhibit multiple subsystems having multiple lengths and time scales. Reliable predictions of such systems need conscious coordination and integration of experiment, theory, and computer simulation. The challenge is to increase predictability by creating a robust design with reduced sensitivity to any influencing variable. A characteristic of future development will be simulation-driven product development (Fig. 35.2), where repeated tests are eliminated to cut the time and cost.

Numerical and experimental techniques are interchangeably used in simulating complex natural phenomena. In the past, scientists such as Leonardo da Vinci, Galileo, and many others adopted experimental techniques to obtain solutions to complex problems whereas continuum mechanics methods would lead to partial differential equations. Many argue that, in the future, numerical techniques will take over the discipline of experimental techniques to solve so-called not-so-complex problems. This seems like the end of the road for a fading discipline. In the past, considerable efforts were made towards the development of knowledge based on actual testing of structural systems. Most of these test results were used to validate predictive models. Validating a predictive model based on experimental test data is not an efficient use of resources. Instead, simulation-driven predictive models will be developed with minimal involvement of experimentation. Structural testing would be imperative for problems that are qualified as either an unknown or important situation.

Future structural systems will be active, intelligent, and adaptive, similar to live biological structures. Live

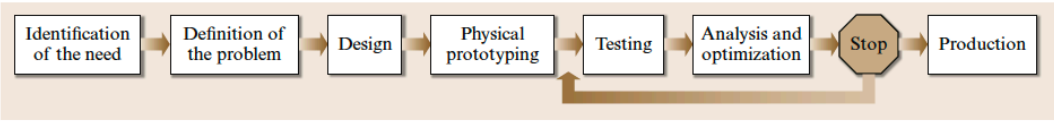

Fig. 35.1 Design-by-testing methodology process flowchart

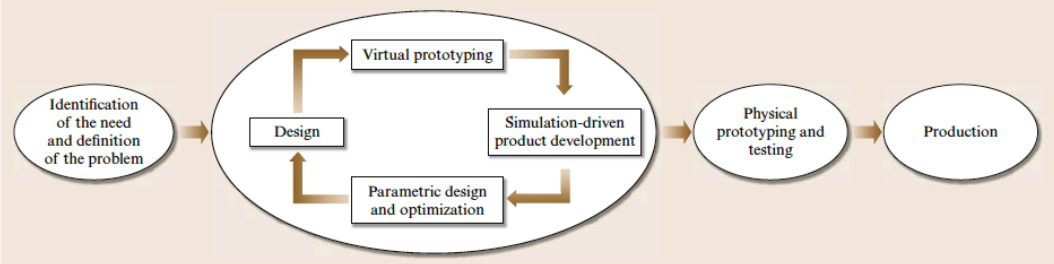

Fig. 35.2 Simulation-driven product development process flowchart

in this context means that these structures will have characteristics like build-in sensors, being adaptive to the prevailing environment, and self-diagnostics and self-repairing/healing. Understanding biological complexity requires sophisticated approaches to integrating scientists from a range of disciplines. These include biology, physics, chemistry, geology, hydrology, social sciences, statistics, mathematics, computer science, and engineering (including mechanics and materials). These collaborations cannot be constrained by institutional, departmental or disciplinary boundaries. The NSF is in the process of initiating a model-based simulation (MBS), which integrates physical test equipment with system simulation software in a virtual test environment aimed at dramatically reducing product development time and cost [35.1]. MBS will involve combining numerical methods such as finite element and finite difference methods, together with statistical methods and reliability, heuristics, stochastic processes, etc., all combined using supercomputer systems to enable simulations, visualizations, and virtual testing. Expected results could be less physical testing or, at best, strategically planned physical testing in the conduct of research and development (R&D). The manufacturing of the prototype Boeing 777 aircraft, for example, was based on computer-aided design and simulation.

The training of engineers and technicians in testing and laboratory activities has decreased significantly since the 1960s due to reduced funding. Funding available for conducting tests, acquiring and maintaining equipment, and developing new techniques continues to decrease, and yet more detailed information is expected from the limited testing performed. Thus, it is absolutely imperative to plan the test program so that it is possible to understand the system from the minimum number of tests performed.

This chapter deals with different aspects of modern ST, where the material used is inert and the loadings applied are conventional. This chapter will start with a discussion of the past, present, and future of structural testing in Sect. 35.1 with some historical illustrations on structural testing; salient features of structural testing that are characteristic of the past will be touched upon. Section 35.2 covers the management approach to structural testing, describing guidelines for planning and performing tests. A generic description of the test equipment and types of measurements is included. Section 35.3 consists of three case studies.

Case study 1 describes modeling for high-strain-rate and high-temperature steel behavior in the National Institute of Standard and Technology (NIST) World Trade Center (WTC) investigation. A major part of the investigation was the metallurgical analysis of structural steel recovered from the two WTC towers. The case study highlights the challenges faced in terms of cataloging the recovered steel to characterize the failure modes, quantifying the temperature excursions that the recovered steel experienced, and characterizing and modeling its mechanical properties.

The second case study highlights how management plays a crucial role in the planning of a major testing program funded by the World Bank. The planning phase provides the basis for a manageable and high-quality testing process. The project involves testing of concrete highway bridges.

Case study 3 details the development of a lightweight automobile airbag from inception through innovation to engineering development. The study demonstrates the engineering progression of the design and the role that testing and analysis played in the development. New test and analysis methods were developed as required during the engineering phase as the design was eventually completed and qualified. This case study also illustrates the close ties between structural testing and numerical simulation.

35.1 Past, Present, and Future of Structural Testing

A structure can be a large system (building, bridge, ship, or aircraft) or it can be something as small as a mechanical robotic actuator or an electronic component made to perform multiple functions; for example, a building structure has the primary function of withstanding loads (self-weight/dead, superimposed/live, wind, seismic, etc.), while providing the users with safety and comfort from the effects of external loads, from shock and vibration, acoustics, thermal, radiation, etc. The building is also required to be aesthetically pleasing. Through testing, the response of the structure under applied loads (force, pressure, temperature, shock, vibration, and other loading conditions) is determined. It is also common for a structure to be required to fulfill new, different or extended functions after it has been designed and built. Most structural testing is considered

to be an art performed by experienced engineers who are familiar with the structure, who will then evaluate and interpret the test results based on their knowledge and experience as much as through prescribed procedures and formulae. In this chapter, an effort is made to present this knowledge of structural testing in a systematic manner.

The history of documented structural testing is as old as the time of Leonardo da Vinci's tensile strength test. The test involved loading iron wires of different lengths. Leonardo da Vinci used a setup similar to the one shown in Fig. 35.3. He used wires of similar diameter and different lengths to suspend the basket (b) from an unyielding support (a). The basket was filled slowly with sand, fed from a hopper (c) with an arrangement so that, when the wire breaks, a spring closes the hopper opening.

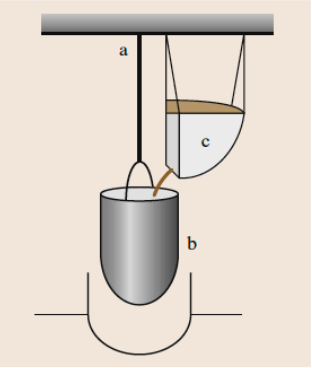

Fig. 35.3 Test setup used by Leonardo da Vinci (see text)

Da Vinci experimentally recorded the failure loads for different length wires. He observed that longer wires were weaker than shorter wires. Early investigators of the time had no explanation for this observation based on the concept of the classical mechanics of materials. What was true for steel as observed by Leonardo da Vinci in the 15-th century is true today for any engineering material. The compressive strength of concrete cylinder (length/diameter = 2), a heterogeneous material, shown in Fig. 35.4, clearly demonstrates the same phenomenon [35.2].

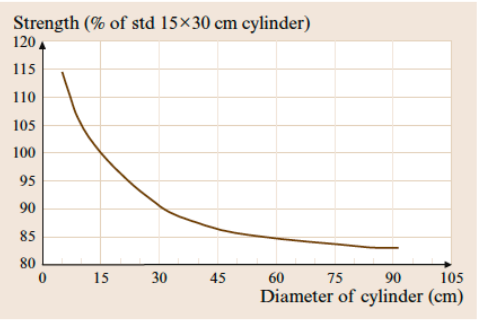

Fig. 35.4 Concrete cylinder under compression

Galileo Galilei demonstrated how structural shape and geometry can influence load-carrying capacity. He arrived at the correct conclusion that the bending strength of a rectangular cantilever beam is directly proportional to its width but proportional to the square of its height. After Galileo came the English physicist Robert Hooke, who observed that the force with which a spring attempts to regain its natural position is proportional to the distance by which it has been displaced. Around the same time, a group of mathematicians and physicists contributed to concepts of force, mass, and formulations of the principles of effect and counter effect. Towards the end of the 17-th century, the first theoretical investigations were carried out on the static behavior of vaults, which is among the most important elements of contemporary engineering structures. The next noteworthy work was that by Leonard Euler, who published an exhaustive treatise on plane elastic curves (bending lines).

Knowledge of the properties of building materials has gradually developed into an important branch of engineering science. In the later part of the 18-th century, numerous strength tests, mainly compression of stone and mortar and bending tests with iron-reinforced stone beams, were carried out by a large number of scientists. Thanks to the ceaseless research work of untold, able engineers with theoretical backgrounds, the methods of structural analysis have since been steadily perfected and extended to new tasks. The knowledge base generated through these efforts has contributed to the development of numerous predictive models. No-one contributed as much as Navier did in the later part of 18-th century and early part of the 19-th century. In his project for the suspension bridge over the river Seine, *Navier* [35.3] carefully selected the material and designed the shape of the anchors based on actual calculations of mechanics Fig. 35.5.

In the past, structures were often developed before the principles of engineering mechanics were understood. The era of theoretical mechanics followed the era of applied mechanics, and personalities such as Poisson, Cauchy, Lamé, Saint-Venant, and many others contributed to the growth of the knowledge base on the theory of structures.

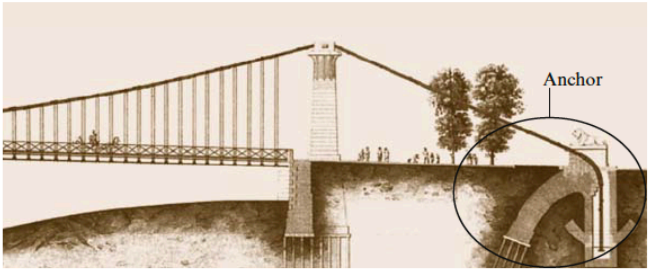

Fig. 35.5 Navier's concept for anchoring the cable (see text)

The Industrial Revolution in England transformed the whole world with coal, steam engines, and railways. Great Britain was the first country to produce iron and steel in large quantities. With improved quality (high strength, elasticity and uniformity) came improved economy, as engineers could determine the dimensions of the structural elements very accurately. With the invention of the hydraulic binding agent called *cement* by Joseph Aspdin came the age of cement and reinforced concrete. During the 19-th century, the dimensions of structures were generally determined so that the admissible stress, calculated on the basis of Hooke's law, was limited to a certain fraction of the breaking stress (the safety factor). It was found, however, that the safety factor thus defined did not represent a reliable measure of the actual safety of the structure, especially for indeterminate structures and structures made with concrete and masonry. With the statically indeterminate structures, however, the local application of a stress beyond the elastic limit will generally lead to a compensation of forces, inasmuch as overstressed parts are relieved by the action of less heavily stressed members. It is obviously only with the aid of extensive tests that these highly complicated conditions can be clarified. There are other problems connected with the strength of materials, which are impossible or difficult to solve on the basis of the classical methods of the mathematical theories. Among these problems is the concentration of stresses, which occurs in complex structural elements in the immediate vicinity of abrupt changes of cross-section, where the concept of stress optics can be ideally applied.

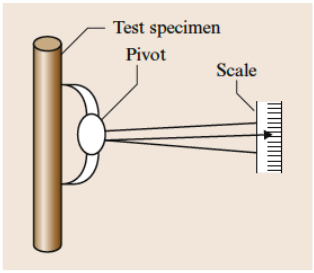

Fig. 35.6 Capp's single-lever extensometer

As far as measurement devices are concerned, for a long time experimentalists from all over the world developed various methods independently without any standardization. Capp's single-lever extensometer [35.4] was one of the early measurement devices of surface strains (Fig. 35.6). For more information on the theory and application of various kinds of extensometers see Chap. 13.

The next generation of extensometers were mounted with mirrors replacing the moving pointer of the rack-and-pinion system, resulting in greater accuracies. They were difficult to calibrate, sensitive to vibrations, bulky, and had restrictions on where they could be mounted on the structure or specimen. Other optical methods are the moiré method (for surface displacement), photoelasticity (for complicated assemblies and parts), brittle coating (for surface crack pattern), holography (for in-plane displacements), speckle pattern (for online monitoring of surface deformation), and digital image correlation.

Earlier descriptions of mechanical measurements of displacement showed the use of mechanical gages. The first electrically based displacement measurement system was the linear variable differential transformer (LVDT). It was not until the invention of electric resistance strain gages and their application in various devices that experimental mechanics began to have a great impact on the design of structures.

Most technologies associated with structural testing have been revised or improved in the past few decades; several new technologies have also been introduced. Portable equipment has been developed, permitting field investigation of a wide range of potential problems with capabilities to perform complicated tests

under adverse conditions. Most of the data-mining methods/techniques are discussed in Parts B & C of this handbook. Despite encouraging results from simulation and predictive modeling, industry is still far from reaching the point where it can discard experimentation. Testing remains an important activity, and its success depends on judicious choice of testing method, instrumentation, data acquisition, and allocation of resources.

35.2 Management Approach to Structural Testing

Test purposes and evaluation criteria are the necessary guides in planning and performing tests as well as the basis for interpreting the test results. For any type of structural testing the activities can be grouped into three phases

- Phase 1, planning and control
- Phase 2, test preparation
- Phase 3, execution and documentation

An important part of testing is the effort spent during the planning and preparation. As a rule of thumb, the distribution of efforts is 20% for planning, 40% preparation, and 40% for the actual execution and documentation of the test program. This means that, during the creation of the functional specification, a master test plan is established. The master test plan describes who performs which type of test and when these tests are performed. On the basis of the agreed test plan, more detailed test plans are made. It is worth noting that there may be legal or regulatory requirements that must be considered while planning for such tests.

35.2.1 Phase 1 – Planning and Control

The planning and control phase starts during the specification of the functional requirements. The planning phase provides the basis for a manageable and high-quality testing process. After the test assignment has been approved, the test team is to be assembled carefully and the test strategy is defined. Manpower selection is crucial for successful outcomes from the testing program. Most testing requires specialist knowledge and skills and the accompanying education to derive high-quality results. A test team typically consists of personnel belonging to a large variety of disciplines. Adequate participation of testing specialists is essential, both in the area of test management and in the area of testing techniques. Test strategy is basically a communication process with all parties involved, trying to define the parts and allotting the necessary time frame. The aim is to have the most feasible coverage of the testing organization and to define the test infrastructure. The objective of the next part of this phase is to manage the progress of testing with regard to the time and resources used. In accordance with the test plan, the testing process and the quality of the test object are documented and reported. The most important deliverable of a test program is a quality test report which also describes the accompanying risks. From the start of the testing process, testers develop a view of quality. It is important that quality indicators are established during all phases of the testing process. Periodically, and when asked, management receives a quality report on the status on the testing process to decide if the testing should be continued or discarded. Major issues that influence the decision-making process during this phase are described in the following subsections.

Safety Requirement

Potential hazards associated with conducting structural tests can be introduced anywhere from a minor source such as electrical shock to a major source like the failure of a hoisting crane, the snapping of a prestressed tendon during tensioning, or the inhalation of toxic fumes. Insights into safety-related issues can be very useful during the planning stage. There are many agencies and regulations such as the Occupational Safety and Health Administration (OSHA) [35.5]), the National Environmental Policy Act (NEPA) [35.6], and the Resource Conservation and Recovery Act (RCRA) [35.7]) that enforce safety laws in the workplace.

Accuracy and Resolution

Some types of tests (e.g., modal analysis) often require many cycles of testing to develop statistically sufficient insights into structural behavior. Test quality is defined through two parameters, obtaining sufficient information to describe structural response, and verifying that the information obtained is valid. A well-executed structural test provides objective evidence of structural behavior.

Specifications (Requirements of Code)

Codes and specifications are developed to bring standardization to experimentalist all over the world. Structural testing has been profoundly affected by the development of codes and specifications. The American Society for Testing and Materials (ASTM [35.8]) has developed test procedures for various kinds of materials. There are organizations who develop test procedures and specific requirements for structural testing. The American Railway Engineering Association (AREA [35.9]), the American Association of State Highway Transportation Officials (AASHTO [35.10]), and the American Institute of Steel Construction (AISC [35.11]) are a few. The way a technique is applied depends on the way the specifications are structured. Based on the testing strategy and the development documentation, appropriate test specification techniques are selected and tailored during the preparation phase. Chapter 17 of the International Building Code 2003 (IBC [35.12]) deals with structural tests and special inspections. Where proposed construction cannot be designed by approved engineering analysis, or where the proposed construction does not comply with the applicable material design standard, the system of construction or the structural unit and the connections shall be subjected to the tests prescribed in section 1714 [35.12].

Classification of Structural Testing

There are different ways in which structural testing can be classified: full scale and models, calibrations, acceptance or quality assurance types, proof tests, material characterization, etc. These tests are aimed to determine stiffness or load deformation, energy absorption, strength or failure load, vibration mode or other structural characteristics.

Full-Scale Test. Characteristics of a structure are influenced by many parameters such as material (nonhomogenous) properties, construction and fabrication techniques, load environment, boundary conditions. The influence of these parameters is not linear, thus making prediction of scaled models difficult. When possible, full-scale structural tests are recommended for accurate prediction of the characteristics of the system.

Load Test. The purpose of conducting load tests is usually to prove that a structure or its components can withstand the anticipated loads. For example, a highway bridge is designed to withstand a particular traffic load. Through load tests on the actual structure, this value can be determined. Section 35.3.2 deals with the load test of a bridge structure.

Destructive/Failure Test. Often tests are carried out to understand the failure characteristics of a structure. Failure tests also indicate the reserve strength and deformation capabilities in a structure. Destructive testing is performed to gain knowledge of the failure modes. At present, the knowledge base of the structural response to a blast load is not well established. To develop design criteria, destructive tests are performed to understand how a structural system will respond to blast loads. Once this design basis is established, computer simulation will replace future destructive testing to save time and cost.

Partial Load Test. Often, samples are taken from the test structure in order to understand the characteristics of the material used for the structure. This test is performed when it is necessary to predict the behavior of the structure, but the design and construction drawings are not available or have changed. More on this type of testing is presented in Sect. 35.3.2.

Nondestructive Test. Nondestructive tests are done to understand the elastic response of a structure and can be classified into diagnostic and proof tests. In a diagnostic load test, the selected load is placed at designated locations on the structure and the response of an individual member of the structure is measured and analyzed. During a proof load test, a structure is carefully and incrementally loaded until the structure approaches its elastic limit. At this point, the load is removed and the maximum applied load (the proof load) and its position on the structure are recorded.

Scaled/Model Test. Full-scale tests are time and resource intensive. Often, scaled tests are done to predict the behavior of a structure by extrapolating observations based on scaled/model tests. There can be serious concerns with any scaled test, and the output should be properly analyzed to arrive at a proper prediction. Sometimes these concerns can be addressed by conducting a series of tests with different scale factors to determine the relation of the observed behavior with size; for example, modal analysis (mode shapes and frequencies) can predict how a structure will store deformation energy under a given loading condition. Modal analysis judgment and experience give insight

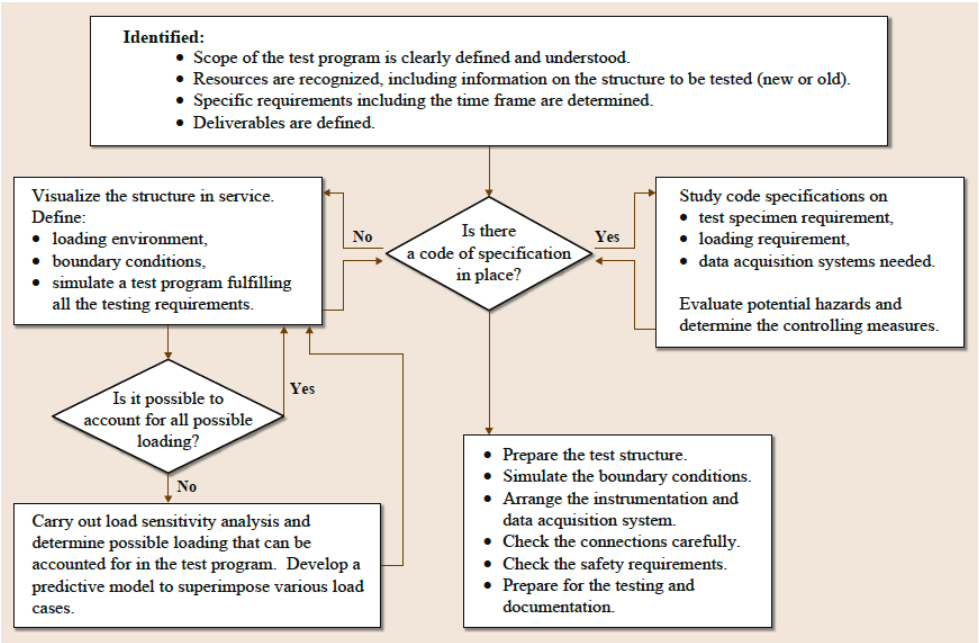

Fig. 35.7 Flowchart of the test preparation during phase 2

into the dynamic response of a structure or component and avoid instability.

To perform a modal test, the test item must be excited (naturally or artificially) in the same manner as the structure would vibrate in different modes. The response to the excitation can be measured by the conventional transducers, which were discussed in Parts B & C of this Handbook. A typical modal test includes an array of accelerometers placed on a structure and connected to amplifiers and a data recording system. An excitation can also be fed to the recording system to collect simultaneous data. Thus a modal analysis is often used to troubleshoot a vibrating system.

Material Test. Structural testing and materials testing must both be considered to construct an accurate predictive model. For material testing, specimens should be extracted from similar structures to be analyzed. Chapters from part B & C of this Handbook contains detailed descriptions of various conventional tests that are performed to characterize materials used to build the structural system.

Forensic Tests. Forensic tests are performed to understand the real cause of any failure of a structure. Failure is a quick phenomenon to which a number of factors contribute. Analysis of such a phenomenon is very challenging. Forensic tests that determined the sequences of various phenomena that contributed to the eventual collapse of the Twin Towers are highlighted in Sect. 35.3.1.

The output of the planning and control phase is a statement or description of the work to be performed based on a feasibility study. Feasible means that a test is possible on the basis of availability of resources, such as manpower, funding, equipment, management tools, and time. This phase will also clearly define

- the tests to be performed
- the available resources
- the specifications (administrative, legal, codal and safety) to be met
- the output and information on the quality and accuracy of the results

35.2.2 Phase 2 – Test Preparation

After the planning and control phase, preparation for actual tests will start. In this phase a systematic study is carried out to understand the test program and deliverables to ensure preparation for a specific test will be thorough and adequate. The structure to be tested is to be designed and developed as if it was a new structure. In the case of an existing structure, the test structure will be identified. Figure 35.7 shows the flowchart of the test preparation during this phase.

Loading on Structure

The loading conditions used in the laboratory and field tests should simulate the service or use conditions. Often, equivalent static loads are used to adequately represent and simplify some complex dynamic environment. In addition to the magnitude of loading, the point of application and the directions are factors that influence any testing program. When the structural system behaves linearly, it is possible to apply loading sequentially. Again, for a linear-elastic system, it is possible to determine the forcing functions mathematically from the measured responses.

Dead Load

Dead loads do not typically change with time, or they change so slowly with time that they produce only static responses. Dead loads include the weight of the structure and loads arising from any permanently attached elements. Dead loads can be accurately estimated knowing the dimensions and density of the elements.

Superimposed Load

Loads that are temporary in nature come under the superimposed load category, like the weight of people in a building. Loads due to wind, earthquake, vibration of moving vehicles, etc. are treated as live or superimposed loads. Often transient loads that arise from impacts, gusts, and other rapidly varying loads are accounted for by additional multiplying factors. Based on safety and serviceability requirements, multiplying factors for the building structure are recommended in the International Building Code (IBC) 2003 [35.12]. When these values are not available, laboratory tests can be conducted to determine them.

Thermal Load

Simulations of thermal loading are rather complex, especially when full-scale tests are conducted. Case study 1 illustrates the challenges encountered while modeling the behavior of structural steel under high temperatures due to the combustion of the aircraft fuel inside the Twin Towers before their collapse. The towers were subjected to dead loads, imposed loads, thermal loads, and impact loads all at the same time.

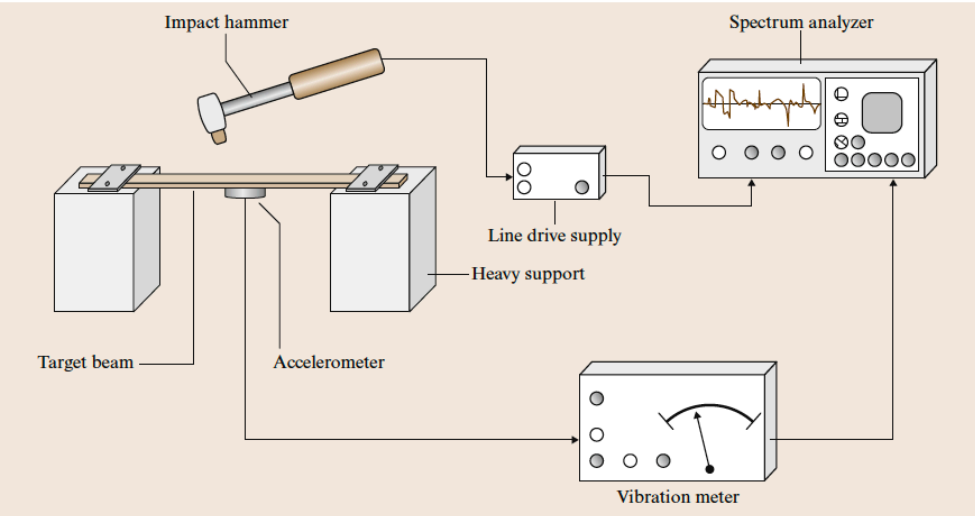

Fig. 35.8 Schematic diagram of vibration test setup

Chapter 7 of the IBC 2003 deals with construction requirements for fire-resistance design for materials used in structures. ASTM E119 contains the necessary test procedures for fire testing.

Dynamic/Vibration Load

Dynamic testing is a widely accepted test method to characterize a structure and its components subjected to time-varying loads. The structure is excited at varied frequencies to determine the proof load, damping characteristics, dynamic modulus, mode shape, etc. Figure 35.8 shows a schematic of a typical experimental setup used to obtain dynamic characteristics of laminated composite beams under an impact load. Vibration of the beam causes the support to vibrate, which in turn influences the vibration of the beam. Thus, for proper interpretation of the test observation, the coupling effect between the support motion and the structure should be carefully accounted for.

Blast and Explosive Load

After the 9/11 terrorist attacks on the Twin Towers, the importance of investigating structures under blast loads has intensified. Blast loads create waves in the air which impact on exposed structures. Loading systems for blast waves and explosive detonations usually require special facilities. Even for very small quantities of explosives, rugged facilities are needed to contain, or at least focus or direct, the released energies. The overpressure/duration relationship for a high explosive or nuclear explosion in air is shown in Fig. 35.9, where p is overpressure (or air blast pressure) and t is time.

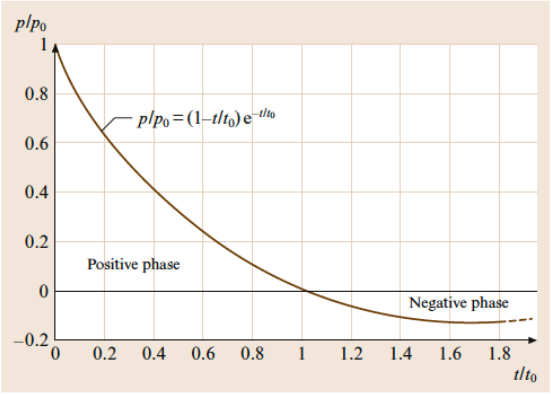

Fig. 35.9 Blast load–duration relationship

In the figure, the decay of pressure after the first instantaneous rise is expressed exponentially. The value of the peak instantaneous overpressure p_0 will depend on the distance of the point of measurement from the center of the explosion. In a TNT (trinitrotoluene) explosion, p_0 might be 200 psi (1.38 MPa) or 300 psi (2.07 MPa) at the point of burst of the explosion, but would rapidly diminish with distance. In a nuclear explosion equivalent to 1000 tonnes of TNT, the peak overpressure would be 2000 psi (13.78 MPa) at 30 m from the center of the explosion.

When an explosive charge is detonated in contact with or very close to a structure in air, the loading can no longer be considered uniform over the area of component faces. The accurate measurement of dynamic loads on structures is a demanding subject. The physical properties of blast waves as they strike the structure are most commonly recorded in terms of pressure. When an explosion occurs within an enclosed room, the impulse that loads the structure may be broken into two distinct parts, the shock front and a quasistatic gas pressure load. This initial blast load is due to the primary shock front and secondary reflected shock fronts. Air shock loadings typically have very short time durations, but may have peak pressures of several thousand pounds per square inch (1 psi = 689.47 Pa) or more. At later times, the structure is loaded primarily by a low-intensity long-duration *gas impulse* that is due to the expansion of the explosive byproduct gases within the structure.

Recording the pressure and acceleration data is a challenge by itself. High-speed photography (typically 2000–3000 frames per second or higher) is also used to measure structural response.

Wind Load

The design and development of a structure that will be exposed to wind loads for most of its service life will usually be tested in a wind tunnel to understand the response of the structure. Aerodynamics plays an important role in the design of an aircraft, automobile, or a high-rise building. The Tacoma Narrows suspension bridge collapsed due to loss of rigidity because of a 42 mph (18.78 m/s) wind, even though the structure was designed to withstand winds of up to 120 mph (53.64 m/s).

Probabilistic Loads

It is well known that structures and material characteristics are seldom known deterministically. This phenomenon was observed by Leonardo da Vinci in the 15-th century, and is still true today. Degrees of

uncertainty in determining material characteristics call for probabilistic approaches to determine the strength of material (as illustrated in case study 2).

Loading Systems

Loading systems are used to apply loads during structural testing. The objective is to replicate service load as nearly as possible. It is very difficult to create exact loading situations in the laboratory, and thus approximations must be made.

Simulation

Consider the simplest situation of applying a uniformly distributed load (UDL) on a plate structure. Figure 35.10 shows at least three ways one can achieve a UDL on a plate structure. The UDL remains uniform as long as the plate does not deform excessively. As soon as the plate deforms, the curvature effect will make the load nonuniform. While trying to simulate UDL, careful consideration is needed to make sure that the UDL is accurately represented throughout the loading history. One way to account for this difference between true UDL and simulated UDL is by adjusting for curvature effects in the response. Thus, it is important to check the method used to apply the loads. This check includes the locations, directions, and manner of applications (point, line, distributed, or inertial). It should also include loading rates and other time-dependent descriptions of the loading, such as magnitudes as the test progresses.

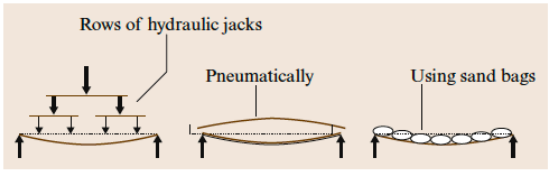

Fig. 35.10 Application of uniformly distributed loads can be done different ways, all of which are different when the beam starts to bend excessively

Loading Equipment

Testing machines are mechanical systems with various controls, including manual, mechanical/hydraulic, and electrical control with feedback systems. Two basic types of controls have the ability to impose either loads or displacements. An excellent description of test control systems is provided in [35.4]. Three main types of force testing machines have been developed and are in use – the dead weight, screw-driven, and hydraulically actuated. Primarily, there are two ways to control loading conditions (interaction between diagnostic and feedback).

1. An open system: performing tests in which the operator retains all the control on loading/unloading and the loading rate
2. Closed-loop systems: performing tests under an environment where the machine controls loading/

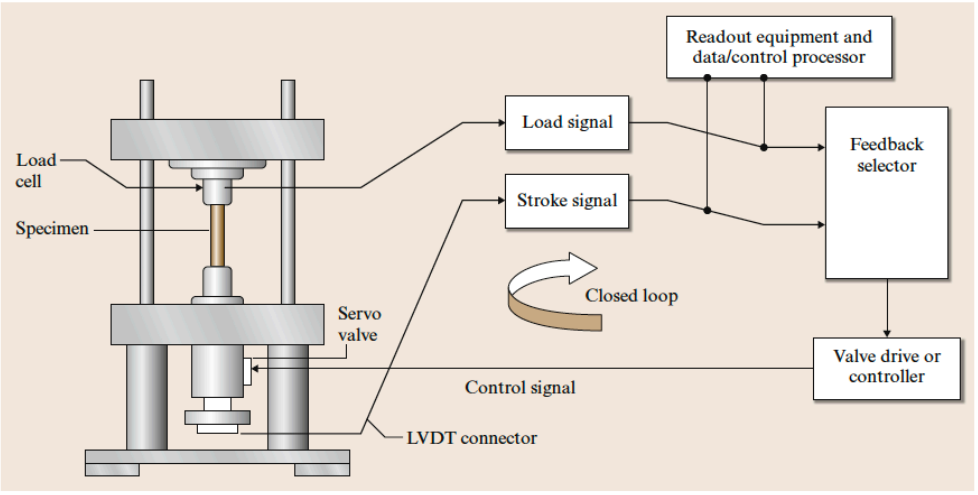

Fig. 35.11 Components with connections for a closed-loop control system

unloading and the loading rate. However, the operator retains a manual override option. A simple block diagram of a closed-loop actuator with a servo–valve combination system is shown in Fig. 35.11.

Calibration

Measurement processes depend on the calibrations of the instruments used. Inconsistent calibrations are common and should be determined in any testing program and the proper corrections should be applied in the response data. By performing periodic checks, one can determine inconsistency in instruments behavior. Often, the instruments used for measurements could be the source of undesirable responses in a testing program. Calibration activities are essential in structural testing because they give credibility to the data generated.

Test Control

There are many ways to apply control and feedback systems in structural testing. It is important to select the proper test equipment to match the requirements.

35.2.3 Phase 3 – Execution and Documentation

In order to satisfy the agreed delivery schedule, the execution phase should start as soon as the preparation for the test program is complete. Sometimes, it may be necessary to conduct exploratory tests to determine the test domain. There are other times when part of the data is used to support a later part of the testing process. The difference between the actual test results and the expected results can indicate a problem area. This can be due to some error with the infrastructure, an invalid test case, or poor judgment. During the entire test execution stage, one should allow for quick and reliable reporting. Possible questions to be addressed are what percentage of the program is complete, how do these tests compare with the prediction, what are the trends, should testing be continued, etc. The infrastructure for testing includes all facilities and resources needed for structural testing. The selection of the correct infrastructure is strongly dependent on the type of resources and hardware platform available.

Obtaining Data

There are wide ranges of transducers, gages, sensors, and other measuring equipment available, as described in Parts B & C of this Handbook. The purpose of a transducer is to convert the physical changes occurring in a structure due to applied loading into an electrical change, usually by altering voltage or current. There are transducers that provide a point response of the structure and there are others that represent full-field or whole-field results. Judicious selection of the testing machine, the right kind of sensors to collect data, and proper processing tools will yield the expected results. Often it is expected to combine both point and full-field techniques to better understand the response of the structure.

Point Techniques. Measurement devices such as strain gages, capacitance gages, load cells, accelerometers, and thermocouples are used to collect structural response in terms of accelerations, displacements, forces, velocities, temperatures, and strains. Response data obtained through the point technique are then fed into an analytical model to analyze the response of the whole structure. For more information on these techniques, refer to Chap. 12 for strain gages.

Full–Field Techniques. This technique examines a portion of the structure or at times, the whole structure. Most of the optical methods provide full-field structural response. The use of such methods (moiré, holography, speckle, photoelasticity, brittle coating, optical-fiber strain gages, thermoelastic stress analysis, or x-ray analysis) prevent the use of another method in the same test. The theories behind most of the full-field techniques are provided in Chaps. Chapter 29 (optical methods), Chapter 20 (digital image correlation), Chapter 21 (geometric moiré), Chapter 22 (moiré interferometry), Chapter 24 (holography), Chapter 23 (speckle methods), Chapter 25 (photoelasticity), Chapter 14 (optical fibers), Chapter 26 (thermoelastic stress analysis), and Chapter 28 (x-ray stress analysis).

Instrumentation and Data Acquisition and Processing

The term instrumentation encompasses all the devices used to sense, connect, condition, display, and record the data. Selection of the instrumentation system is dictated by the requirements of the loading environment. For more information, refer to [35.4, Chap. 10].

Data Transmission. To avoid hazards in many test situations, sensitive instruments and personnel can be located remotely. Thus the cables that connect transducers with the signal conditioner and recorder should be such that their signal attenuation is minimized. This

attenuation is more pronounced in the case of high-frequency signals.

Signal Conditioning. Once a mechanical response is sensed, the output of the sensor needs to be amplified for use in the recorders. This is known as signal conditioning, and is done after the response is converted into an electrical signal.

Computer Data Acquisition. This topic is covered exclusively in ([35.4, Chap. 10]).

Completion Phase

The completion phase is launched after the execution phase is completed. These activities are generally less structured or often forgotten, and when under high pressure, concessions are made. There should be some provisions on how to carry out additional tests (if so warranted) after evaluating test results based on the main test program.

Experimental Methods – Evaluation Criteria. Test evaluation criteria consist of methods according to which test results can be interpreted and understood. Evaluation criteria are usually specified through methods and techniques of engineering mechanics and material science. The data obtained from the associated measurement devices used in testing will make correlations and comparisons of theory and test data more direct and easier to understand. Rarely do test results and theoretical predictions agree completely, even more so in the case of a complicated system. Much of the time needed for a test setup is used to ensure that the loading conditions are realistic, while attempting to comply with the test purposes and evaluation criteria.

On rare occasions, when large discrepancies between theoretical predictions and test results occur, the experiment is systematically debugged in the following order:

1. Questions will arise about the validity of the calibration of the instruments, i. e., the relationships between known inputs and observed outputs and the uncertainties associated with the two measurement processes are quantified and defined;
2. Questions will arise on the signal conditioning and data acquisition;
3. Questions will arise about the capabilities of the test personnel.

It is better for everyone to get involved and discover the problem as early as possible in the laboratory or under controlled conditions.

35.3 Case Studies

After careful selection, three case studies have been included in this chapter on structural testing. The first study is based on modeling aspects of high-rate and high-temperature tests on steel retrieved from the collapse of the World Trade Center disaster. This study only highlights the issues that were not addressed in earlier chapters. This investigation falls under forensic study. The next case study deals with the challenges faced while conducting nondestructive and load tests on multiple concrete highway bridges. The third case study illustrates how structural tests can innovate a product design.

35.3.1 Models for High-Rate and High-Temperature Steel Behavior in the NIST World Trade Center Investigation

Description

In September 2002, the NIST became the lead agency in the investigation of the World Trade Center (WTC) disaster of September 11, 2001. That investigation addressed many aspects of the catastrophe, from occupant egress to the factors that affected how long the Twin Towers stood after being hit by the airplanes [35.13,14]. A major part of the investigation was the metallurgical analysis of structural steel recovered from the two WTC towers. The analysis included tasks to catalog the recovered steel, characterize the failure modes of the columns, quantify the temperature excursions that the recovered steel experienced, and characterize and model its mechanical properties. The last task consisted of two major subtasks:

1. Assess the quality of the steel recovered from the collapse site to ascertain whether it had the yield strength called for in the design drawings, and determine whether its properties were consistent with those expected of construction steels from the WTC construction era.
2. Provide material models for room-temperature stress–strain behavior, high-strain-rate stress sen-

sitivity, and high-temperature plasticity and creep behavior to the groups that conducted the finite element modeling of the collapse sequence [35.15].

This case study summarizes the findings and methodologies of the second subtask.

Challenges and Strategy

Challenges. The team faced five challenges in completing the subtask of the metallurgical analysis:

1. Very little of the structural steel from the fire and impact floors remained when NIST assumed control of the investigation. Although the salvage teams recovered many important perimeter columns from near the area of impact in WTC 1, most of the structural steel was recycled very soon after the excavation of the site.
2. Identifying and cataloging the recovered steels was extremely time consuming. After the recovered columns arrived at NIST, team members attempted to identify their locations in the building using the original structural plans and various remaining identifying marks.
3. The WTC towers were constructed from a much wider variety of steels than is common in high-rise building construction. Unlike many tall buildings, which might use only three or four grades of steel supplied to ASTM specifications, the WTC employed 12 yield strength levels, many of which were proprietary grades from foreign steel mills. Four different fabricators, who purchased steel from both domestic and foreign mills, worked on the fire and impact floors alone. The wide variety of steels made it impossible to completely characterize each one.
4. Locating suitable areas to harvest test coupons was frequently difficult. The collapse and subsequent recovery efforts damaged many of the columns by plastically deforming them. Truss elements proved extremely vexing in this regard. Not only were their original locations in the building unidentifiable, but they were compressed into tight balls for removal from the collapse site during the recovery. This handling rarely left any material suitable for mechanical testing.
5. The accelerated time schedule necessary to deliver evaluated properties to the modeling groups frequently required the team to evaluate properties using literature values, even when recovered steel existed in the NIST inventory.

Strategy. To evaluate the quality of the steel and to establish baseline mechanical properties, the group tested at least one tensile specimen from each yield strength level. Additional specimens from relevant steels from the fire and impact zones were also characterized. To characterize the high-rate stress sensitivity, the focus was on perimeter and core column steels from near the impact zone. These columns were most relevant for determining the severity of damage to the buildings caused by the impact of the aircraft. To characterize the high-temperature deformation behavior, the focus was on steels from core columns and the floor trusses. Creep characterization focused on the floor truss steels only. In parallel to the experimental characterization, the team developed methods to estimate properties of other steels not characterized, using literature data and models as well as test results on WTC steels.

Test Methods

Room-Temperature Tensile Tests. Evaluating the quality and establishing the baseline tensile behavior of the steels from the fire and impact zones required several hundred room-temperature tensile tests that encompassed all the relevant strength levels and forms, such as plates, rolled shapes, and truss components. The test protocol generally followed ASTM E 8 (and in some cases ASTM A 370) for comparison to mill-test report data. All tests retained the extensometer on the specimen past the point where the specimen began to neck to capture the full stress–strain behavior. Results of these tests were used to assess the quality of the steel, as well as to form the basis of the stress–strain models for the high-rate and high-temperature behavior.

High-Strain-Rate Tests. Relevant steels from the impact zones were tested at rates up to $500\,s^{-1}$ to establish the strain rate sensitivities of their strengths. The test suite comprised eight perimeter column steels with $50\,ksi \le F_y \le 100\,ksi$ ($345\,MPa \le F_y \le 689\,MPa$) and five core column steels with $36\,ksi \le F_y \le 42\,ksi$ ($248\,MPa \le F_y \le 290\,MPa$). The core column group included examples of both plates from built-up box columns and wide-flange shapes. Specimens from both shapes were machined from sections flame-cut from the original columns. Specimen gage sections were located at the one-half or one-quarter depth positions (as required by E 8 and A 370) and well away from any flame-cut edge. Tension tests in the range $50\,s^{-1} \le \dot{\varepsilon} \le 500\,s^{-1}$ employed a servohydraulic test machine with a special slack adapter grip that allowed the actuator to reach full speed before loading the specimen [35.16].

The gage section of the typical test specimen was 32 mm long; the cross section was 6.35 mm × 3.17 mm. This specimen was geometrically similar to the larger, standard tensile specimen used in the quasistatic tests, which allowed pooling of the data for evaluating the effect of strain rate on ductility. In the high-strain-rate tests, the specimen stress was measured by using a strain gage bonded to the nondeforming grip end of the specimen, while the specimen strain was measured from a high-elongation gage bonded to the gage section. The 1% offset yield strengths YS_{01} for all tests were evaluated using the European Structural Integrity Society (ESIS) procedure, which is described graphically in the inset to Fig. 35.12 [35.17]. Choosing the 1% offset yield strength YS_{01} instead of the more common 0.2% offset YS_{002} removes most of the spurious effects from load cell ringing, which can be misinterpreted as increased strength.

High-Temperature Tests. Two types of tensile tests characterized the high-temperature behavior of representative specimens of steels from perimeter columns, core columns, floor trusses, and truss seats. A first group of standard, high-temperature tensile tests, which followed ASTM E 21, complemented the room-temperature tensile tests and formed the basis for the high-temperature plasticity models. In general, the high-temperature tensile tests employed round specimens with $d = 12.7$ mm. Strains were measured on a 25.4 mm gage length. Test temperatures were 400 °C, 500 °C, 600 °C, and 650 °C, which spans the temperature region where the strength changes most rapidly. To maximize the number of different steels tested and define the temperature dependence of the strength, generally only a single test was made at each temperature. A second group of short-time creep tests characterized the time-dependent deformation behavior of steels from the floor trusses. These tests employed smaller specimens, with a 32 mm-long uniform cross-section that is 6.0 mm by 3.17 mm. Characterizing the creep behavior required about 20 tests per steel, at the same temperatures used in the high-temperature tensile tests.

Deformation Models

High Strain Rate. High-strain-rate tensile tests, as displayed in Fig. 35.12, show the strain-rate sensitivity of the steels. Although several models exist for describing the change in strength with strain rate, a particularly simple one is

$$\sigma = \sigma_0 K \left(\frac{\dot{\varepsilon}}{\dot{\varepsilon}_0} \right)^m , \tag{35.1}$$

where the strength σ can represent the 1% offset yield strength YS_{01}, for example. Figure 35.13 plots the calculated strain rate sensitivity m of the 1% offset yield strength YS_{01} for the perimeter and core column steels.

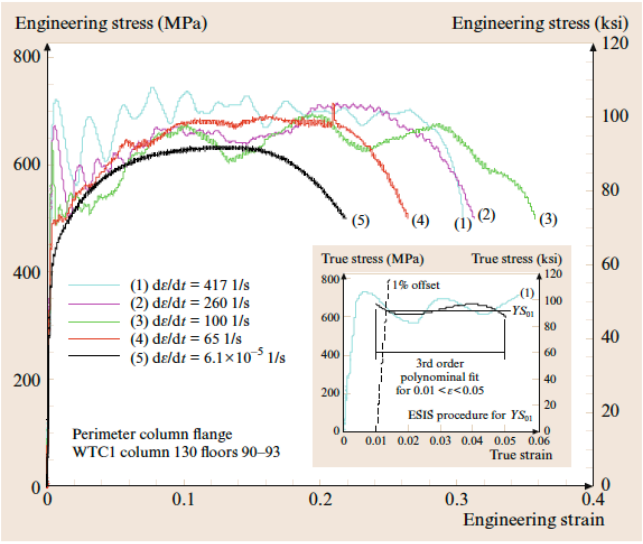

Fig. 35.12 Example stress–strain curves for high-rate tensile tests. The *inset* describes the procedure for estimating the 1% offset yield strength YS_{01}

The plot also includes the strain-rate sensitivities calculated from the reported yield strengths for some other construction and low-alloy steels from the WTC construction era [35.18–24]. The strain-rate sensitivities of the yield strength of the WTC steels are similar. The accelerated delivery schedule for the strain-rate sensitivity data required that the team supply a single strain-rate sensitivity for all steels, which was evaluated using a subset of the steels in Fig. 35.13. Because that strain-rate sensitivity was based primarily on data from the higher-strength perimeter column steels, it slightly overpredicts the strength increase of the lower-strength core column steels. Significantly, none of the perimeter column steels suffered from brittle failure at the high deformation rates expected from the aircraft impact. At rates of up to 500 s^{-1}, the total elongation to failure El_t was never less than 20% for any of the steels characterized.

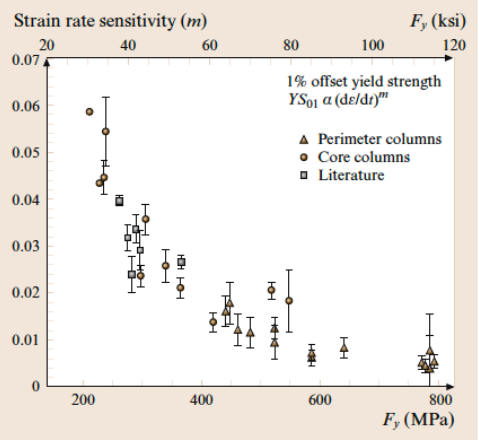

Fig. 35.13 Strain-rate sensitivity m of the 1% offset yield strength YS_{01} for WTC steels and structural steels of similar strength and composition

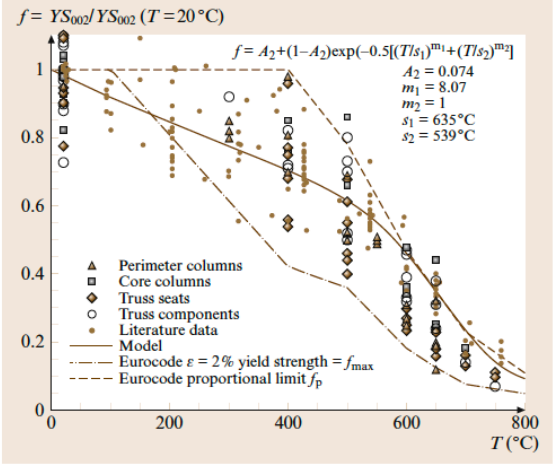

Fig. 35.14 High-temperature yield strength YS_{002} for steels recovered from the WTC, structural steels from the literature and the model for the normalized yield strength f

High Temperature. NIST supplied three models for calculating the high-temperature behavior of the relevant steels from the fire zone:

1. normalized yield and tensile strength as a function of temperature
2. tensile stress–strain (plastic) behavior as a function of temperature
3. creep strain as a function of temperature, stress, and time

Figure 35.14 compares the measured 0.2% offset yield strength YS_{002} of the recovered steels to a suite of literature data for structural steel [35.25–31].

The solid line represents the model for the temperature dependence of the yield strength, which was developed from the literature data in Fig. 35.14 before significant testing was complete. The data for the WTC steels generally lie slightly below the bulk of the literature data for $T > 500\,°C$, probably because the WTC tests employed a slower testing rate.

In addition to the generic yield and tensile strength behavior model of Fig. 35.14, NIST developed a second set of models to predict the stress σ as a function of strain ε and temperature T for all steels in the fire zone

$$\sigma = R_{TS}\,K(T)\varepsilon^{n(T)}\,. \qquad (35.2)$$

The temperature-dependent terms in this stress–strain model account for the decreasing work hardening with increasing temperature. The form of the functions $K(T)$ and $n(T)$ is the same as the master curve for high-temperature normalized yield strength in Fig. 35.14. The accelerated delivery schedule required NIST to develop models for all relevant steels based on test data from only two steels. The behavior of A 36, $F_y = 36$ ksi (248 MPa) steels was estimated from literature stress–strain curves [35.25]. The behavior for all other steels, including the wide-flange core column in Fig. 35.15, is

based on the stress–strain response of nominally ASTM A 242, $F_y = 50$ ksi (345 MPa) micro-alloyed steel recovered from the WTC floor trusses.

To calculate the stress–strain behavior of an uncharacterized steel, the stress is scaled by the ratio, $R_{TS} = TS_{ref}/TS$, of the room-temperature tensile strength of the reference steel on which the model was developed to the tensile strength of the uncharacterized steel. Scaling by the room-temperature tensile strength TS produced greater fidelity than scaling by the ratio of room-temperature yield strengths, as previous studies have done [35.32]. Figure 35.15 compares the stress–strain curves at different temperatures for specimens from the flange of a wide-flange core column to the prediction of the global model of (35.2). Note that the parameters used to predict the stress–strain curves were developed using data from the ASTM A 242, $F_y = 50$ ksi (345 MPa), micro-alloyed truss steel, and not the plotted wide-flange core column steel. The quality of the prediction confirms the choice to scale the results by the ratio of the room-temperature tensile strengths, R_{TS}, in (35.2).

The third set of models NIST supplied included two models to represent the creep behavior of all the different steels exposed to the fires. The first, for the low-strength A 36 steels, came directly from previous NIST research, and was based on literature data for the creep of low-strength structural steel [35.32, 33]. The second model, used for all other higher-strength steels, was based on the creep data from the ASTM A 242, $F_y = 50$ ksi (345 MPa) micro-alloyed steel recovered from the WTC floor trusses. Both models broke the temperature T, stress σ, and time t dependence of the creep strain ε_c into separate functions

$$\varepsilon_c = A(T)\,(R_{TS}\sigma)^{C(T)}\,t^{B(T)}\,. \qquad (35.3)$$

The exact forms of $B(T)$ and $A(T)$ differ slightly between the two models.

Like the high-temperature stress–strain models, the difference in creep response of the various steels was captured by scaling the stress by the same tensile strength ratio R_{TS}. An extensive comparison of the results of this method on a suite of literature data sets for creep of structural steel established the superiority of this method over two other possible scaling ratios, no scaling and room-temperature yield-strength scaling [35.34, 35]. No scaling of the applied stress (i. e., setting $R_{TS} = 1$) is equivalent to assuming that all steels have identical creep behavior. Scaling the stress by the room-temperature yield strength ratio proved to be particularly unsuitable. Creep curves from this method deviated the most from the literature experimental data.

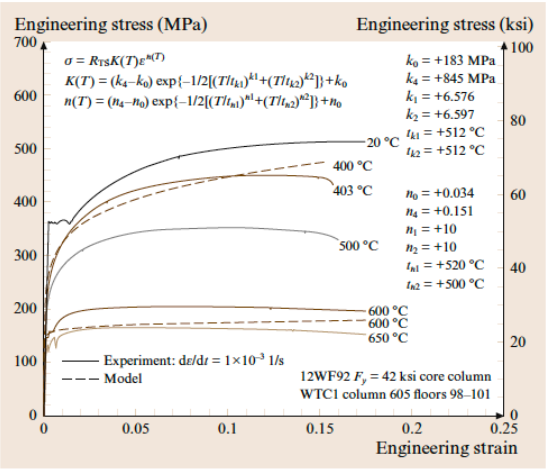

Fig. 35.15 High-temperature stress–strain curves and the prediction of the global model (35.2) for high-strength steel

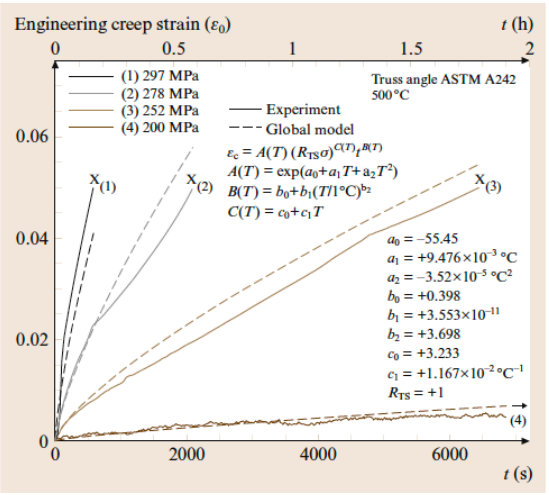

Fig. 35.16 Creep curves and the prediction of the global model (35.3) for creep of floor truss steels that conformed to ASTM A 242

Figure 35.16 compares the experimentally determined creep curves for the $F_y = 50$ ksi (345 MPa) micro-alloyed floor-truss angle steel to the prediction of the global model in (35.3).

This shows the excellent fidelity of the prediction of the global strain–time model for that steel. However, because NIST did not characterize the creep response of any other WTC steels, it is not possible to assess the fidelity of the prediction on the WTC steels.

Summary

NIST conducted more than 500 mechanical property tests to assess the quality of the steels and develop material models in support of the World Trade Center collapse investigation. These data supported models for room-temperature stress–strain behavior, strain-rate sensitivity, and high-temperature deformation. The case study highlights the challenges faced in terms of cataloging the recovered steel to characterize the failure modes, quantifying the temperature excursions that the recovered steel experienced, and characterizing and modeling its mechanical properties.

35.3.2 Testing of Concrete Highway Bridges – A World Bank Project

Introduction

The National Highways Development Project (NHDP) launched in 1999 was India's largest ever highways project, covering a length of nearly 24 000 km (15 000 mile). The project cost (estimated to be US $25 billion) was funded by the World Bank, the Asian Development Bank, and the Indian Government [35.36]. The objective of this project was to develop a world-class highway network with uninterrupted traffic flow. A large part of this network involves improving the existing system, which was constructed during the 1950s. Most of the bridges in these highways had signs of distress due to lack of regular maintenance, and in most cases, records on their design and construction details were nonexistent. The traffic on these structures had increased dramatically since their original construction. This situation called for tests to estimate the load-carrying capacity, particularly to determine if they had developed material deterioration and loss of section strength over the years of usage. Due to budget and time constraints, only a few bridges could be completely tested and assessed. This case study describes how the management approach, explained in Sect. 35.2, was implemented to test a large number of bridges within the constraints of time and cost.

Challenges Involved

The investigating team came across three major challenges in completing this project.

1. Test structures were located on National Highways that connect different states. The traffic volume on these highways is very high. Even for testing purposes, highway closure for more than 15 min was not permitted. Thus a testing method that allowed intermittent loading, allowing normal flow of traffic between two successive tests, was adopted. Intermittent loading is possible only by using articulated trucks. A market survey demonstrated that no such test truck with a telescopic working platform existed in the country (Fig. 35.17). Importing such a truck was not feasible from the perspective of cost and time.
2. Most bridges had visible distress marks and had no design/construction documentation available. As a result, a number of additional tests (mostly nondestructive and partial destructive) had to be performed to determine the characteristics of the concrete. It is a well-established fact that no single

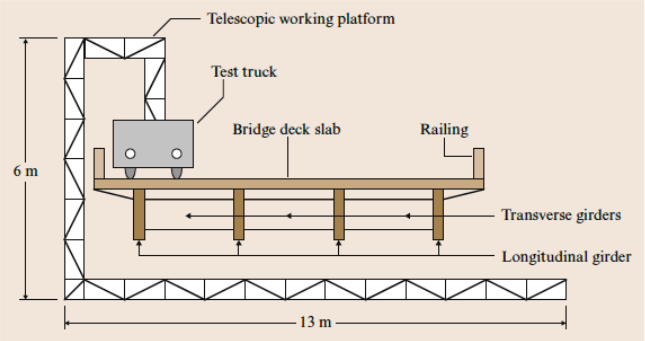

Fig. 35.17 Test truck with telescopic working platform

test would be sufficient to assess the condition of any of these structures.

3. The greatest challenge was developing a theoretical model to predict the load–deflection behavior of a distressed structure. This model was needed during load testing of the highways.

Planning and Control Phase

In order to meet the objectives of the test program, it was necessary to test these structures in three phases.

Phase 1 – Visual Assessment. Visual assessment was carried out in order to detect all symptoms of damage and defects as per specifications given in a special publication (SP) of the Indian Road Congress (IRC:SP-35) [35.36]. A carefully selected assessment team, represented by experts from each of the contributing agencies (i. e., funding agencies, users, consulting firms, and the state highway department) were involved during this phase. On the basis of visual assessment, all of the bridge structures were categorized into three groups

- Group 1 – bridges with little or no distress at all, which were not recommended for testing
- Group 2 – bridges with minor distress, which were recommended for testing to determine the severity of the distress
- Group 3 – bridges having considerable distress, for which tests were not needed as their replacement can be clearly justified

Bridges that fell into group 2 were identified and grouped, and only representatives from each group were recommended for testing. The objective of this test program was to

- evaluate safe load-carrying capacity and
- establish a common procedure for posting a structurally deficient structure.

Phase 2 – Generation of a Scientific Database. Since there were no design/construction related data available, this phase was adopted to generate following information:

- physical/geometrical information of various elements;
- a map of crack (structural or nonstructural) patterns existing in the structure;
- characteristics of the concrete used in various elements of the structures – this was done by conducting nondestructive and partial-destructive tests;
- A theoretical model to predict the response of the structure.

Phase 3 – Load Testing. Load testing of the actual bridge structure was performed to ascertain the live load-carrying capacity. The procedure for rating the live load capacity requires knowledge of both the actual physical condition of the bridge and the actually applied loads. This phase involves the following tasks:

- Task 1 – Based on the traffic survey report and following the specification given in IRC:SP-37 [35.37], the test load was determined. Load test was done at four different stages of loading as given in the procedure. The chosen loading arrangement should be such that these values can be achieved quickly. Sand bags, which can be added or removed easily, were used to achieve the required loading.
- Task 2 – Fig. 35.18 shows the distribution of sand bags to achieve the code-specified axle-wise load distribution.
- Task 3 – Before conducting the actual load test, a theoretical model was developed to predict the de-

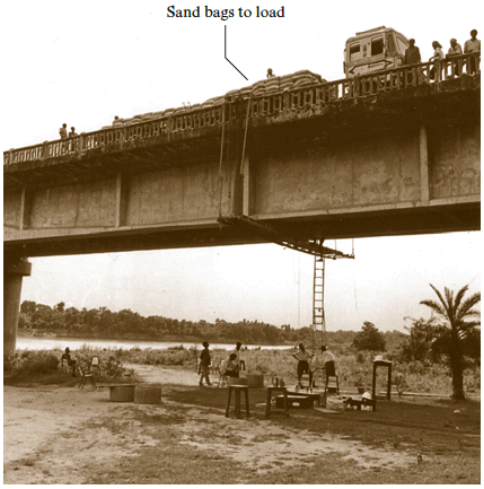

Fig. 35.18 Sand bags used to achieve code-specified load with the proper distribution

flection of the structure at various stages of loading, assuming
  - dead load of the transverse girders as concentrated loads
  - twisting of the transverse girders due to eccentrically-applied live loads (in the form of the influence factor of the girder)
  - railing dead load, as a uniformly distributed load (UDL)
  - Deck slab and girders constructed monolithically (i. e., longitudinal girders worked like T-beams)
  - Prestressed concrete longitudinal girders, originally designed as balanced sections with the soffit stress due to self-load as $-5\,kg/cm^2$, and the profile of the tendon was assumed to be parabolic.
- Task 4 – Actual load test.

After the field tests, a rating analysis was performed and the safety of the bridge structures was determined and reported, after proper documentation.

Preparation

Preparations for the testing program included the following tasks:

- Task 1 – On the basis of the traffic survey, the heaviest vehicle plying on the bridges was determined to be 25 tonnes. The code specifies to use the next heavier vehicle, i. e., an articulated truck trailer of 35.2 tonnes. Figure 35.19 shows the geometry of the test vehicle, along with the axle-wise load distribution to meet specifications of the code. The spatial distribution of the sand bags to achieve different stages of loading was ascertained through proper calibration.

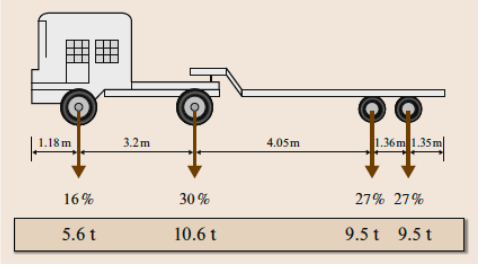

Fig. 35.19 Geometric of the test vehicle with axle-wise load distribution

- Task 2 – The working platform was designed, fabricated, and tested in the laboratory before being transported into the field. The platform was made using rectangular steel tubes in a telescopic arrangement to be easily transported in pieces and assembled at site quickly. Figure 35.20 shows the simple but elegant arrangement of the suspension system for the working platform. Using a proper counterweight, the requirement for a cable at the site was avoided.
- Task 3 – The instruments intended to be used for nondestructive, partially destructive, and load tests were properly calibrated in the laboratory.

Execution and Documentation

The test program constitutes three different kinds of tests:

- Test 1 – Nondestructive tests
- Test 2 – Partially destructive tests
- Test 3 – Load tests

Brief descriptions of each of these tests are given below.

Test 1 – Nondestructive Test. Four subtests were performed under nondestructive tests

1. subtest 1 – to determine compressive strength of the concrete by impact hammer
2. subtest 2 – to determine the quality of concrete using ultrasonics
3. subtest 3 – to determine the reinforcement cover by cover meter
4. subtest 4 – to measure the corrosion of reinforcing steel using a half-cell meter

Subtest 1 – Impact Hammer Test (Also Known as Schmidt Hammer Test or Rebound Hammer). This test indicates the hardness of the concrete surface and indirectly reflects the strength of the concrete. ASTM C 805 provides the necessary specification for this test. Characteristics of this test method are

- a large number of readings can be taken in short duration,
- a large number of locations on the structure can be selected,
- a statistical approach with a high degree of confidence can be applied,
- the actual structure is tested, therefore the test result reflects the totality of the final product,

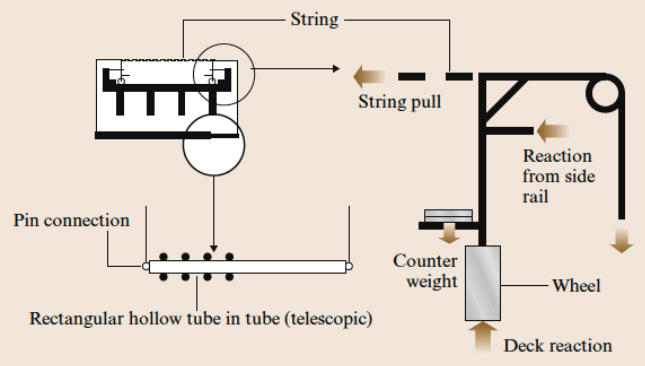

Fig. 35.20 A single arrangement on how the working platform was analyzed, designed, fabricated in the laboratory before being transported to the site for field test

- the strength of concrete in a structure can be determined with an accuracy of ±15%. When little information is available about the concrete quality, the error can be up to ±25%.

ASTM C 805 specifies that ten rebound numbers be recorded for each location. The minimum number of locations where tests should be performed is ten per element. Thus for any element, there are 100 test readings. These are analyzed statistically as: f_{ck} (most probable characteristics strength, MPCS, of concrete) = $f_m - 1.64\,S$, where f_m is the mean value of the strength data and S is the standard deviation (SD) of the data. Figure 35.21 shows the frequency distribution of concrete in the deck slab of the bridge with identification number 38/1.

Subtest 2 – Ultrasonic Test. In an ultrasonic test, compressive strength estimates are derived from time-domain signals. The density of a material affects both pulse velocity and strength. Thus there is a unique correlation between the longitudinal (compressive) wave velocity and material strength. ASTM C 597 outlines this test procedure.

The operational principle of modern testing equipment includes the measurement of longitudinal, transverse, and surface waves. The receiving transducer detects the onset of the longitudinal waves and determines which is the fastest. From the velocity of this pulse, estimation can be made on strength. Table 35.1 gives the classification of concrete on the basis of pulse velocity.

The zero setting of the equipment is done during the calibration of the device. Characteristics of this test method are

- surface condition and moisture content can influence pulse velocity by up to 20%
- existence of cracks in the material has a strong influence
- the presence of steel reinforcement can increase pulse velocity by about 40%
- age, aggregate type, and size of the concrete all influence pulse velocity

Subtest 3 – Cover Test. Major causes for the deterioration of reinforced cement concrete (RCC) structures have been the corrosion of the embedded reinforcement. The main cause for the occurrence of corrosion is identified as the absence of proper cover, which provides the protective shield. When reinforcement details are

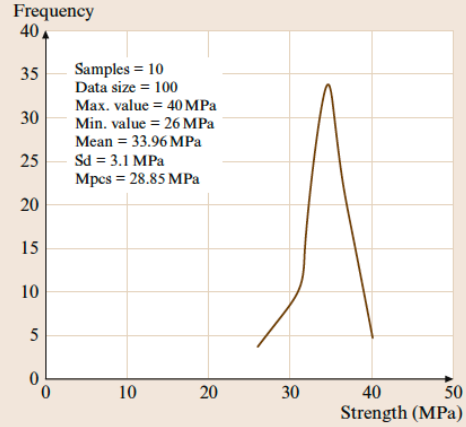

Fig. 35.21 Frequency distribution of concrete strength

Table 35.1 Classification of the quality of concrete on the basis of pulse velocity

Longitudinal pulse velocity km/s	10^3 ft/s	Quality of concrete
> 4.5	> 15	Excellent
3.5 – 4.5	12 – 15	Good
3.0 – 3.5	10 – 12	Fair
2.0 – 3.0	7 – 10	Poor
< 2.0	< 7	Very poor

Table 35.2 Assessment of rate of corrosion

Measured electrode potential	Corrosion rate
< 250 mV	Insignificant
> 250 mV and < 350 mV	Corrosion initiated
350 mV	Corrosion is certain
> 350 mV	High to severe

not known, the position of the reinforcement close to the surface can be determined by a cover meter. A cover meter has a probe and an indicator on the front panel. The position and direction of the reinforcement embedded in the concrete were determined by sweeping the probe symmetrically over the surface. The needle of the indicating instrument will deflect if the probe nears a reinforcement bar. This is measured by placing the probe in different positions until a maximum needle deflection is obtained.

Subtest 4 – Corrosion Test. When reinforcing steel is embedded in concrete, it does not normally corrode. The inherent cement-alkaline environment acts as a *protective passive layer* on its surface. However, if the depth of cover of the concrete is insufficient, then the passive layer can break in the presence of excessive amount of chloride ions. The chloride can originate from sodium chloride (common salt) in marine locations or from de-icing applications, or from the use of a particular admixture, e.g., calcium chloride (accelerator), or from surrounding soil, from the contaminated unwanted aggregates themselves or even from the mix water or curing water. The breakdown of the passive layer will force the steel to rust and expand in volume. As a result, the concrete cracks.

In order to assess the rate of corrosion of embedded steel in concrete qualitatively, half-cell potential measurement, an electrochemical nondestructive technique, was adopted for the detection of the state of re-bars within the concrete structure. The procedure for this test is to divide the surface under test into a grid system of suitable dimensions as per site conditions. Intersections of these grid lines are marked numerically as shown in Table 35.3. Assessment of the rate of corrosion on the basis of half-cell potential is given in Table 35.2. ASTM C 876 has the necessary specifications for this test.

Test 2 – Partially Destructive Test. Of all the tests available for the determination of compressive strength of concrete, a core test may be the most direct test of in situ concrete. In this test method, cylindrical cores are cut using a rotary diamond drill (ASTM C 42) from the candidate structure and then polished and tested under uniaxial compression. While identifying a location for core cutting, regions where embedded reinforcement steel is present should be carefully avoided.

Cores can be used to determine not only the compressive strength of concrete but also some of the other characteristics of the structure, i. e., carbonation depth, cement content, chloride content, and sulfate content in the mortar (ASTM C 1084). The presence of excessive chloride and sulfate in the concrete can cause corrosion of the embedded reinforcement. The process of drilling, including the vibration and impact, can weaken the interface between the cement paste and the aggregates. Core testing has an accuracy of approximately ±12% if a single core is tested. If multiple cores are tested at the same location, the mean core strength will have an accuracy of $\pm\sqrt{(23/n)}\%$, where n is the number of cores [35.38]. Table 35.3 shows typical core test observations.

Test 3 – Load Test: Deflection Prediction. From the available geometrical and material data, a theoretical model is developed. Theoretical deflection is due to both the self-weight of the structure and the superimposed load due to the truck trailer loaded with sand bags.

Equation (35.4) gives the deflection due to a uniformly distributed dead load of intensity w.

$$y = \left(\frac{1}{EI}\right)\left(-wLx^3 - wx^4 - 0.0416wL^3x\right). \tag{35.4}$$

As per IRC SP 37 [35.39], the position of the truck-trailer should be such that it causes the absolute maximum bending moment in the girder. The bending moment under the load will be at the absolute maximum when a load and the resultant of the set of loads are equidistant from the center of span for the various possible combinations of loads. When more than one truck-trailer are used, as per the code spec-

ification, the clear distance between vehicles CD is 18.5 m. Figure 35.22 shows the longitudinal placement of two truck-trailers, one completely inside the span, i. e., DEFG and the other partially, i. e., ABC on the span.

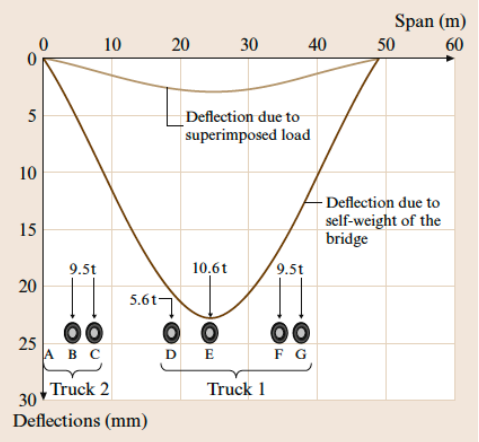

Fig. 35.22 The longitudinal placement of two truck-trailers as per code specification

For this position of live loading, deflection can be found by the method of superposition given by equations (35.5,35.6) as

$$y = \left(\frac{1}{6EI}\right) \left[-P(L-a)x^3 + Pa(L-a)(2L-a)x\right], \quad \text{for } x < a, \tag{35.5}$$

$$y = \left(\frac{-Pa}{6EI}\right) \left[\left(\frac{(L-x)^3}{L}\right) + \left(\frac{(L^2-a^2)x}{L}\right) - (L^2-a^2)\right], \quad \text{for } x > a. \tag{35.6}$$

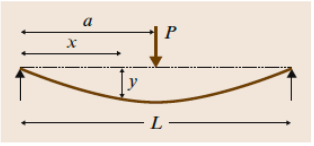

Fig. 35.23 Deflection of a simply supported beam due to a concentrated load P at mid span

Total deflection can be obtained after combining the live load and dead load deflections.

Procedure for Load Testing. As per the requirement of the code:

- observations are made to find the existence of any cracks. If found, they should be marked and their width should be measured;
- for ease of observation of the behavior of cracks and their new formations during the test, a lime whitewash was applied the day before testing at the critical section;
- the load test was done during the morning hours of the day when the variation in temperature was low.
- the test load was applied in stages of $0.5W$, $0.75W$, $0.9W$, and W, where W was the gross-laden weight of the test vehicle (i. e., 35.2 tonnes);
- for each stage, the corresponding loaded vehicle was brought to the marked position and the observations of deflections was made instantaneously, and again after 5 min;
- after the placement of the load, the development of new crack and the widening of the existing cracks were observed;
- prior to the start of testing, the theoretical deflections at various stages of loading were calculated and plotted. If the in situ deflections exceeded these values by more than 10%, the test was discontinued;
- for testing with multiple test vehicles, the individual vehicles were gradually brought into position and the resulting deflections were continuously monitored;
- the test vehicle was taken off the bridge, and instantaneous deflection recovery and the deflection recovery after 5 min were noted.

Figure 35.22 shows that the deflection caused by self-weight (uniformly distributed over the span) was around ten times that for the superimposed load. Deflection was measured at mid span using a dial gage with a resolution of 0.01 mm.

Rating Analysis. After the load test, a load versus deflection graph is drawn. The load corresponding to a deflection of 1/1500 of the span is determined after extrapolating the load–deflection curve to obtain the acceptance load. Most of the bridges demonstrated nearly 100% recovery of deflection with unloading of the test vehicle. Test observations are summarized in Table 35.3.

Table 35.3 Summary of tests conducted on the bridge identified as no. 38/1 over the River Subarnarekha on National Highway 60

Test	Location of test	Observations	Inference
Test 1,	Deck slab	MPCS 28.85 MPa; SD = 3.1 MPa	Good
Subtest 1	Pier	MPCS 19.37 MPa; SD = 9.12 MPa	Average
Hammer test	Longitudinal girder	MPCS 35.81 MPa; SD = 5.80 MPa	Good
(Strength in	Transverse diaphragm	MPCS 30.85 MPa; SD = 4.14 MPa	Good
MPa)	Pier cap	MPCS 24.88 MPa; SD = 8.01 MPa	Average
Test 1,	Deck slab		Good
Subtest 2	Web of girder		Good
Ultrasonic	Flange of girder		Good
pulse test	Diaphragm		Fair
Test 1,	Soffit of central girder from upstream (U/s) face	30	Adequate as per code
Subtest 3	Web of central girder from U/s	40	Adequate as per code
Cover (mm)	Central diaphragm between central and U/s girder	40	Adequate as per code
	Soffit of deck slab between central and U/s girder	25	Adequate as per code
	Pier no. 2 from west side	55	Adequate as per code
	Pier cap no. 2 west face	60	Adequate as per code
Test 1,	Abutment (2.8 m from top)	1 – 580 mV	Rate of corrosion is very high
Subtest 4	Grid area = 0.09 square meter around the exposed bar as shown on the rightmost cell in Fig. 35.25.	2 – 630 mV	
Corrosion	Distance from 1 to 8 = 600 mm	3 – 640 mV	
intensity	Distance from 1 to 2 = 150 mm	4 – 690 mV	
around an		5 – 688 mV	
exposed bar		6 – 750 mV	
		7 – 594 mV	
		8 – 650 mV	
		9 – 620 mV	

Test 2	Structural element	Strength (MPa)	Carbonation depth (mm)	Cement (%)	Chloride (%)	Sulfate (%)
Partially	Top slab	30.1	Nil	15.41	0.033	0.045
destructive	Abutment cap	28	Nil	10.83	0.009	0.033
test	Kerb	26	Nil	13.33	0.013	0.058
(core test)	Girder	Weak	2	17.91	0.04	0.14
	Upper abutment	Weak	2	11.25	0.1	0.033
	Lower abutment	24	Nil	10.83	0.015	0.055
	Pier	16	1	10.83	0.007	0.065

Test 3	Recovery of deflection	Full recovery	Loading is within the elastic limit
Load test	Rating of the bridge on the basis of load test	The bridge is safe for a class-A train of vehicle, 70R tracked, and wheeled vehicles	

Bridge characteristics:

- prestressed concrete girder bridge with 13 spans ($1\times 21.3+11\times 48.8+1\times 12.5=570.6$ m long) with a cross section as shown in Fig. 35.24. N is the number of transverse girder.

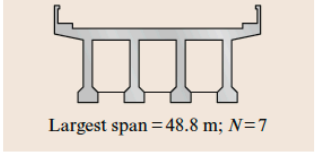

Fig. 35.24 Cross section of the bridge identified as no. 38/1

- visual distress includes spalling, reinforcement bar exposure, and cracks in the deck slab and on supporting structures

Summary of the test observations is given in Table 35.3.

35.3.3 A New Design for a Lightweight Automotive Airbag

Description

In 1991, Sandia National Laboratories and a fabric manufacturing company initiated a project to develop a lightweight fabric automotive airbag. The objective of the project was to address performance issues inherent with incumbent, heavyweight automotive airbags. For example, heavyweight fabric airbags, constrained by imposed pack volume, must be small, necessitating high pressures in the airbag to decelerate the occupant during an accident. Conversely, lightweight fabric airbags could be considerably larger, resulting in lower pressures exerted on the occupant during an accident. Also, the lightweight fabric is soft and smooth, which eliminates the facial abrasion experienced with heavyweight fabric airbags. Finally, the momentum of airbag deployment imparts a large impulse to the occupant's face, a phenomenon termed *face-slap*, which is mitigated by the smaller mass of lightweight fabrics.

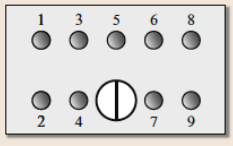

Fig. 35.25 Grid points around the exposed bar as marked numerically from 1 to 9

It was anticipated that a lightweight fabric airbag would require a new design to pass the rigorous testing of an automotive industry component. The incumbent driver-side airbag, a two-piece circular design, is not very structurally efficient. To check this notion, an incumbent two-piece, circular airbag was fabricated using the lightweight fabric and subjected to a burst-pressure test. The airbag industry employs burst-pressure testing to assist in the design qualification of prototype airbags. During this test, the airbag is inflated with ambient air over several seconds until the airbag fails structurally. While each automotive manufacturer requires different qualification standards, the result of the lightweight-fabric, two-piece circular design burst-pressure test conclusively demonstrated that lightweight fabrics would require a new design to produce a viable airbag.

Challenges Involved

Early lightweight fabric prototype designs converged on gore-shaped structures similar to solid-canopy parachutes and hot-air balloons, as depicted in Fig. 35.26. An initial design review concluded that the proposed prototypes might satisfy the engineering specifications, but certainly would not represent a cost-effective, marketable product.

Using cost as the exclusive constraint, a subsequent design session produced a radically different yet economically viable airbag. The simple design used a single square piece of fabric and the enclosure was completed by folding the corners toward the center of the square, as shown in Fig. 35.27. Seams were constructed along the diagonals where the free edges formed, and a hole was cut in the center to accept the attachment hardware. This pattern ensures with its very simple design that the airbag produced the strongest seams and no parent fabric was wasted.

Planning and Control Phase

To prove this design, a significant quasistatic pressurization and dynamic-deployment cold-air inflation test series was initiated. The experimental test lab consisted of a high-pressure source and serially plumbed solenoid valves that could supply a dynamic burst of air simulating an inflator deployment. High-speed video cameras (1000 fps) were the primary diagnostic tools that assisted the post-test evaluation of the early prototypes. Simple pressure-transducer measurements monitored the progress of the evolving prototypes. This enabled the airbag deformation pressure–time history to be quantified during these inflations.

Quasistatic tensile tests of the fabric were performed to determine the ultimate capacity of the fabrics, along with the stiffness, or modulus of elasticity. To correctly determine the modulus, a uniaxial straining of the material is required. *Wrap* grips were used in these tests to wrap the fabric over a cylindrical fixture to avoid the hourglass deformation patterns common with other test fixtures. The crosshead of the test machine in these quasistatic tests moves at a maximum rate of 10 in/min (0.0042 m/s) while the load and deformation are recorded. The modulus was measured along the original fabric roll direction (the warp direction), across the fabric roll direction (the fill direction), and in-between or at 45° to each of these directions (the bias direction). This modulus data is used as the basis of the structural analysis model definitions. Prototype seams were also evaluated using the tensile tests, with construction variables such as seam type, thread size, needle size, stitches per inch, type of stitch, and reinforcement materials.

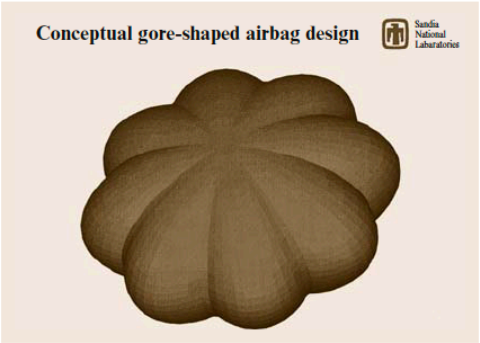

Fig. 35.26 Early prototype design appears to be gore shaped

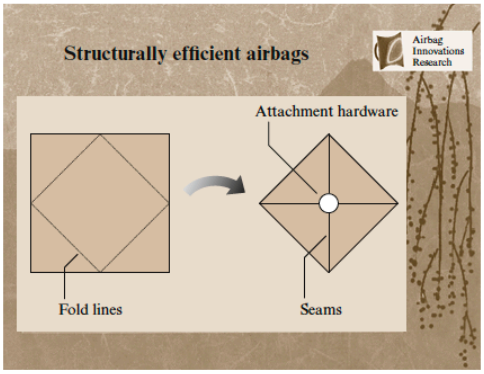

Fig. 35.27 A simple design using square fabric to reduce wastage

Simulation

A structural analysis investigation of the new design was started to understand how load is distributed in the airbag. The chosen approach called for finite element analyses using the nonlinear code Abaqus [35.40]. This code allows for gross deformation of the airbag during inflation using membrane elements that incorporate the orthotropic behavior of the fabric. A simulation of the deployments from the cold-air inflation testing was chosen to allow direct comparisons with a known loading.

High-speed video coverage of the airbag deployments was compared with the deformation from the analyses, showing that the curvatures of the airbags were dissimilar. These analyses used the loading measured as pressure–time histories and the quasistatic material properties described above. The testers conjectured that the inflation dynamics (which occurs in the time frame of 10–20 ms) were altering the effective stiffness of the fabric. Dynamic tests were then justified to determine the strain-rate sensitivity of the fabric.

Postprocessing of the analysis strain showed a strain rate of 5–10 /s in the fabric during the pressurization (analysis is a very good tool for determining the strain rates of loading, and is generally not intuitive). Using this information, tensile tests were designed utilizing a high-speed MTS load frame. This test machine is capable of producing a velocity of 200 in/s (5.1 m/s) in the crosshead. A photograph of this test setup is shown in Fig. 35.28, where a seam test sample is shown in a temperature-conditioning fixture. The gage length of the sample was adjusted until the desired strain rate was achieved, and verified using high-speed video coverage of the test. This was accomplished by running the test machine at its maximum speed and adjusting the test sample length until the desired strain rate was measured using the video coverage. The correct specimen length was iteratively determined by repeating the test until the strain rate of interest was finally achieved. The desired strain rates were bracketed to ensure consistency of the measurements and the loading technique for the test specimen.

Testing at the loading rate of the airbag deployment showed an apparent stiffening of the fabric matrix, and produced as much as a 30% increase in the elastic modulus of the fabric. The strain-to-failure was also

frequently reduced depending on the amount of crimp in the fabric weave (essentially an expression of how tightly the fabric is woven).

There was also a large modulus discrepancy between the fabric construction directions, warp and fill. Warp fibers are the yarns in the direction of the fabric roll, and fill fibers are passed in between and normal to the warp yarns, to make up the fabric matrix. Typical tensile test results of nonoptimized fabrics are shown in Fig. 35.29, where the load–displacement response of the fabric is shown for both the warp and fill directions during high-speed tests.

The complete loading history of the same fabric in the warp and fill direction is shown in the figure (machine startup dynamics occur early in the load trace, as noted) with the actual tensile loading being represented by the second half of the load trace. Note that, not only is the slope or modulus of the material not the same, but the strain-to-failure of the material is different by almost a factor of three. The strength of the fabric is similar in the warp and fill directions (the normal way fabric is designed or ordered). Most importantly, the elastic properties of this material cannot produce a balanced state of strain in the resulting airbag deployment with this mismatch in moduli (the two slopes of the load traces approximated by the lines in the same figure). Future fabric construction for this airbag was designed to balance out the moduli in the warp and fill directions.

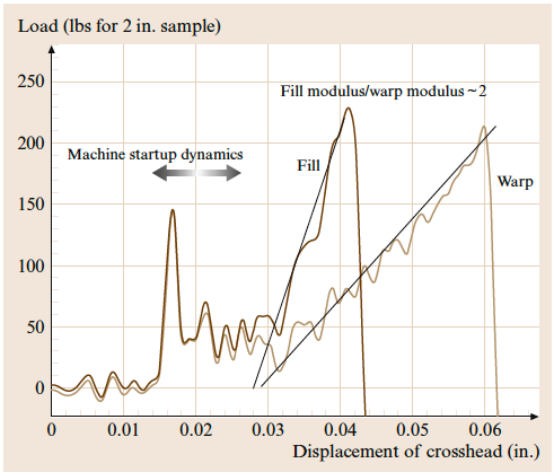

Fig. 35.29 Load–displacement history of fabric in the wrap and fill directions (1 lbs = 4.4 N; 1 in = 2.54 cm)

Validation of the Model

When this new understanding of the fabric properties was incorporated into the analyses, the curvature of the airbag's high-speed deployments improved greatly. A still image during deployment is shown in Fig. 35.30. In this figure, the photo of the airbag is overlaid with the deformed mesh lines (shown in black) of the finite element membrane model. The curvature of the front and rear panels of the airbag now match very well. This proves graphically that the dynamic modulus infor-

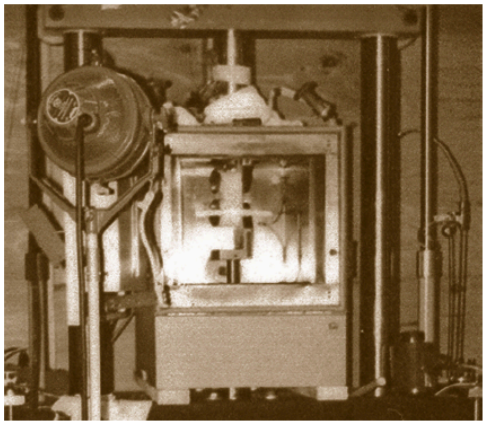

Fig. 35.28 High-speed MTS load frame

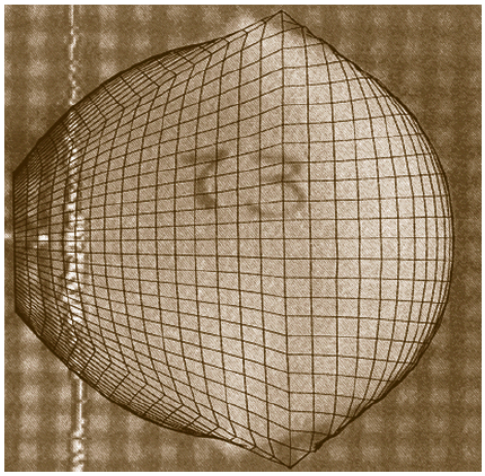

Fig. 35.30 Photograph and analysis overlay of inflated airbag

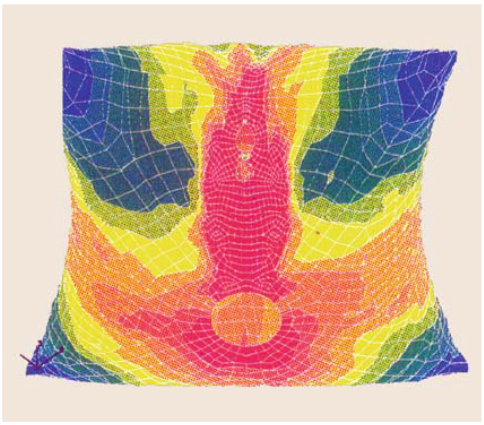

Fig. 35.31 Warp stress distribution of the mounting area of the airbag

mation, replacing the earlier quasistatic tests, produces the correct state of stress and deformation in the fabric structure.

The airbag seams have warp- and fill-directed fabric on opposite sides of the seam due to the geometry and simplicity of the design. Any mismatch in the properties of the warp and fill will cause shear stress to develop at the seam interface. Conversely, shear stress control down the seam line is made easier by the balancing of modulus of the dissimilar directions. Any imbalance in the moduli across the seam must be balanced by producing shear across the seam, which leads to tearing or premature failure. The analyses showed these effects of airbag construction. The warp stress contours around the mounting area of the airbag are shown in Fig. 35.31.

Developing seams to move with the deforming panels of fabric was the next step in project optimization. It is clear that different levels of bunching occur during the loading process due to the different amounts of fabric adjacent to the stitching. This relates directly to the shear stress formation down the line of the seams. This seam behavior was also optimized using the high-speed test frame so that the radii of the stitched material increased the ability of the material to handle the dynamics of the inflation. This seam optimization is an example of an analysis that has identified an issue and its root cause, which was then addressed through testing.

Once the state of stress in the airbag is understood, it is possible to determined how this stress can be balanced across the seams. Moduli balancing was accomplished by literally designing the fabric weave to act in a balanced fashion. Yarns in the fabric weave were removed to achieve a stronger fabric. This was a radical concept to achieve a dynamically balanced fabric response. This concept led to altering the yarn properties in conjunction with the weave design to dynamically and statically optimize the fabric action [35.41].

A case study that details the project from inception through innovation and engineering development has been presented. It was noted that the implementation of different constraints led to radically different design proposals during the innovation phase. The study also demonstrated the engineering progression of the design and the role that testing and analysis played in the development. New test and analysis methods were developed during the engineering phase as the design was eventually completed and qualified.

35.4 Future Trends

In nature, shape and structure spring from the struggle for better performance, thus they are adaptive and multifunctional. Exciting progress is being made in developing engineered systems with ideas taken from the biological world. These systems are complex and call for an interdisciplinary effort encompassing a breadth of science and engineering disciplines, including biological sciences. Living organisms produce a striking array of structural concepts with a wide variety of biological functions. For example, consider the case of a daffodil stem, a biological beam with a high bend-to-twist ratio of ~ 13, while that of an isotropic circular beam would be 1.0–1.5. This natural beam will twist and bend in response to wind loads to reduce drag by up to 30%. Thus, structural testing of a biological beam should incorporate loading under bending and twisting simultaneously. The particular combination of these loading cases will be function of the characteristics of biological structures or materials.

Generating engineering concepts with ideas from the biological world will be the emphasis of future research efforts. The growth of the field (biomechanics, biomimetics, biomaterials, bioengineering, biological soft tissue, etc.) can be seen by its maiden presence in

Chaps. 7, 31, and 32 of this Handbook. More than half a dozen journals specific to biological materials have been started in the last decade. The number of publications in this area during last 5 years exceeds those published during the previous 50 years.

Advances in medical imaging (e.g., 3-D Doppler echo and magnetic resonance imaging), medical image reconstruction techniques, and computer simulation methods are playing important roles in our health care system, both for the design of new medical devices and for the rehabilitation simulators that provide real-time feedback for health-care planning and training. For proper validation of these structural systems, (medical devices and simulators), state-of-the-art measurement, control, and analysis techniques will be needed.

Nanoscale technology will influence the future in many ways. Multifunction nanotubes are wonder material with unusual combination of characteristics: strength (more than 460 MPa), creep resistance, electrical conductivity, damping, and many other desirable characteristics at high temperature (450 °C) through to cryogenic environments. Naturally, a structure developed using this wonder material should be tested in coupled modes. Chapters 16 and 30 of this Handbook contain more information on carbon nanotubes.

References

35.1 R. Sack: *Model Based Simulation* (National Science Foundation, Arlington 1999), White paper, See also: [www.eng.nsf.gov/cms/] for update

35.2 W.H. Price: Factors influencing concrete strength, Proc. J. Am. Concr. Inst. **47**(6), 417–432 (1951)

35.3 H. Straub: *A History of Civil Engineering – An Outline from Ancient to Modern Times* (MIT Press, Cambridge 1964)

35.4 R. Reese, W.A. Kawahara: *Handbook of Structural Testing* (Society of Experimental Mechanics, Bethel 1993)

35.5 H. Erwin: *OSHA 1910 General Industry Standards Made Easy*, 2nd edn. (Erwin Training Institute, Edmonton 1989)

35.6 National Environmental Policy Act under US DOE at http://www.eh.doe.gov/nepa/

35.7 http://www.epa.gov/region5/defs/html/rcra.htm

35.8 American Society for Testing and Materials: http://www.astm.org/

35.9 The American Railway Engineering and Maintenance Association: http://www.arema.org/ (2008)

35.10 http://www.aashto.org/ and http://www.transportation.org/

35.11 American Institute of Steel Construction http://www.aisc.org/

35.12 International Code Council: *International Building Code* (International Code Council, Country Club Hills 2003)

35.13 National Institute of Standards and Technology: *Federal Building and Fire Safety Investigation of the World Trade Center Disaster: Final Report of the National Construction Safety Team on the Collapses of the World Trade Center Towers* (NIST, Gaithersburg 2005), available at http://wtc.nist.gov

35.14 F.W. Gayle, R.J. Fields, W.E. Luecke, S.W. Banovic, T. Foecke, C.N. McCowan, T.A. Siewert, J.D. McColskey: *Federal Building and Fire Safety Investigation of the World Trade Center Disaster: Mechanical and Metallurgical Analysis of Structural Steel* (NIST, Gaithersburg 2005), available at http://wtc.nist.gov

35.15 W.E. Luecke, J.D. McColskey, C.N. McCowan, S.W. Banovic, R.J. Fields, T. Foecke, T.A. Siewert, F.W. Gayle: *Federal Building and Fire Safety Investigation of the World Trade Center Disaster: Mechanical Properties of Structural Steels* (NIST, Gaithersburg 2005), available at http://wtc.nist.gov

35.16 D.M. Bruce, D.K. Matlock, J.G. Speer, A.K. De: Assessment of the strain-rate dependent tensile properties of automotive sheet steels, SAE Technical paper 2004-01-0507 (SAE, 2004)

35.17 European Structural Integrity Society: Procedure for Dynamic Tensile Tests. In: *ESIS Designation P7-00*, ed. by K.H. Schwalbe (ESIS, Delft 2000)

35.18 D. Chatfield, R. Rote: *Strain Rate Effects on Properties of High Strength, Low Alloy Steels*, Publication No. 740177 (Society of Automotive Engineers, Warrendale 1974)

35.19 H. Couque, R.J. Asaro, J. Duffy, S.H. Lee: Correlations of microstructure with dynamic and quasi-static fracture in a plain carbon steel, Met. Trans. A **19**(A), 2179–2206 (1988)

35.20 R. Davies, C. Magee: The effect of strain-rate upon the tensile deformation of materials, J. Eng. Mater. Tech. **97**(2), 151–155 (1975)

35.21 A. Gilat, X. Wu: Plastic deformation of 1020 steel over a wide range of strain rates and temperatures, Int. J. Plast. **13**(6-7), 611–632 (1997)

35.22 J.M. Krafft, A.M. Sullivan: On effects of carbon and manganese content and of grain size on dynamic strength properties of mild steel, Trans. ASM **55**, 101–118 (1962)

35.23 M. Langseth, U.S. Lindholm, P.K. Larsen, B. Lian: Strain rate sensitivity of mild steel grade ST-52-3N, J. Eng. Mech. **117**(4), 719–731 (1991)

35.24 M.J. Manjoine: Influence of rate of strain and temperature on yield stresses of mild steel, Trans. ASM **66**(A), 211–218 (1944)

35.25 T.Z. Harmathy, W.W. Stanzak: Elevated-temperature tensile and creep properties of some structural and prestressing steels. In: *Fire Test Performance, ASTM STP 464*, ed. by ASTM (American Society for Testing and Materials, Philadelphia 1970), pp. 186–208

35.26 R. Chijiiwa, Y. Yoshida: *Development and Practical Application of Fire-Resistant Steel for Buildings*, Nippon Steel Techn. Rep. **58**, 47–55 (1993)

35.27 S. Goda, T. Ito, H. Gondo, I. Kimura, J. Okamoto: Present status of weldable high strength steel, Yawata Techn. Rep. **248**, 5086–5163 (1964), in Japanese

35.28 J.M. Holt: Short-time elevated-temperature tensile properties of USS "T-1" and USS "T-1" Type A constructional alloy steels. In: *United States Steel Report* (Applied Research Laboratory, Monroeville 1963)

35.29 J.M. Holt: Short-time elevated-temperature tensile properties of USS Cor-Ten and USS Tri-Ten high-strength low-alloy steels, USS Man-Ten (A 440) high-strength steel, and ASTM A 36 steel, US Steel Corp. Rep. **57**, 19–901 (1964)

35.30 G.F. Melloy, J.D. Dennison: *Short-time elevated-temperature properties of A7, A440, A441, V50, and V65 grades. Internal memorandum to J.W. Frame* (Bethlehem Steel, Bethlehem 1963)

35.31 United States Steel Corp.: *Steels for Elevated Temperature Service* (United States Steel Corporation, Pittsburgh 1972)

35.32 B.A. Fields, R.J. Fields: *Elevated Temperature Deformation of Structural Steel. NISTIR 88-3899* (National Institute of Standards and Technology, Gaithersburg 1989)

35.33 D. Knight, D.H. Skinner, M.G. Lay: *Short Term Creep Data on Four Structural Steels. Report MRL 6/3 Melbourne Research Laboratories* (The Broken Hill Proprietary Company, Clayton 1971)

35.34 G. Williams-Leir: Creep of structural steel in fire: analytical expressions, Fire Mater. **7**(2), 73–78 (1983)

35.35 M. Fujimoto, F. Furumura, T. Abe, Y. Shinohara: Primary creep of structural steel (SS41) at high temperatures, J. Struct. Construct. Eng. **296**, 145–157 (1980)

35.36 National Highways Authority of India: http://www.nhai.org/

35.37 IRC: SP:35-1990, Guidelines for Inspection and Maintenance of Bridges, Indian Roads Congress (R. K. Puram, New Delhi 1991), http://www.irc.org.in/

35.38 S.S. Seehra: Specimen Testing vis-á-vis in-situ Testing, Nondestructive Testing of Concrete Structures (Indo-US Workshop on NDT, Roorkee 1996)

35.39 IRC: SP:37-1991, Guidelines for Evaluation of Load Carrying Capacity, Indian Roads Congress (R K Puram, New Delhi 1991), http://www.irc.org.in/

35.40 Abaqus Inc.: *Abaqus Users Manual* (Abaqus, Providence 2005)

35.41 K. Gwinn, J. Holder: Fabric with Balanced Modulus and Unbalanced Construction, Patent 0930986B1 (2004)